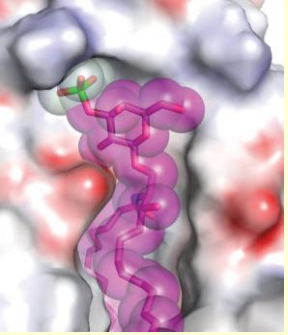

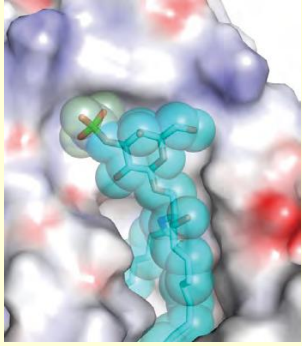

Макромолекулярная кристаллография с синхротронным излучением

А. Попов (ESRF)

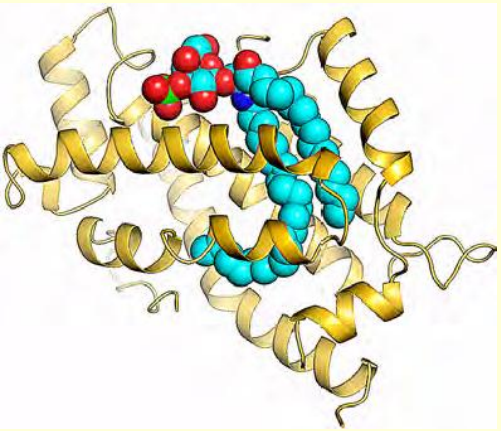

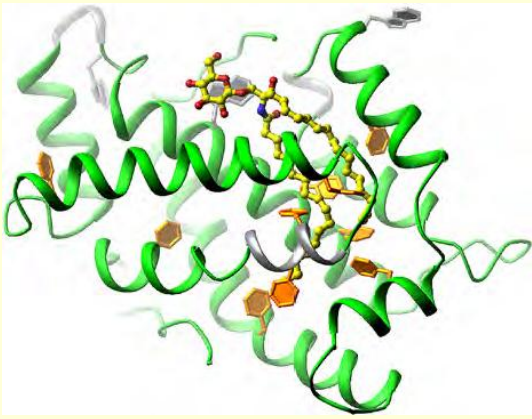

Macromolecular Crystallography is a technique used to study biological molecules such as proteins, viruses and nucleic acids (RNA and DNA) to a resolution higher than ~5 Å. This high resolution helps elucidate the detailed mechanism by which these macromolecules carry out their functions in living cells and organisms.

DNA double helix: A, B, Z

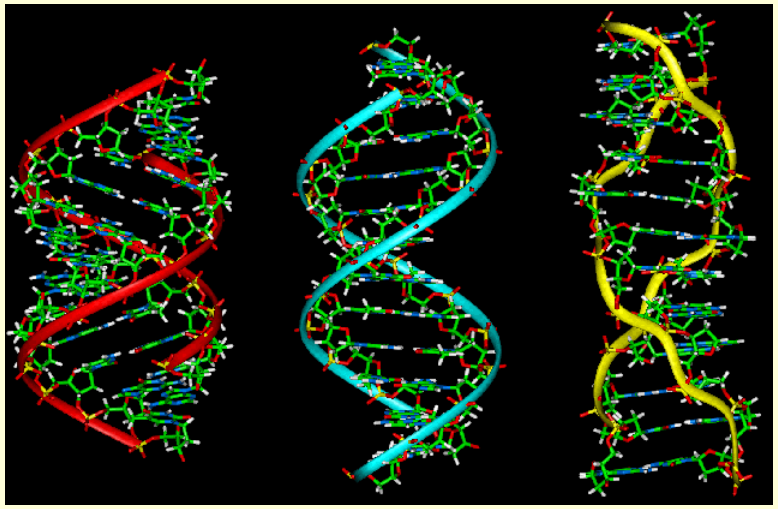

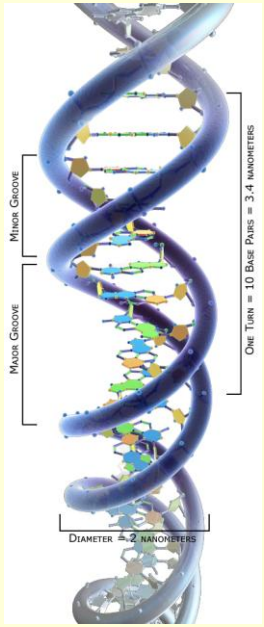

RNA molecules

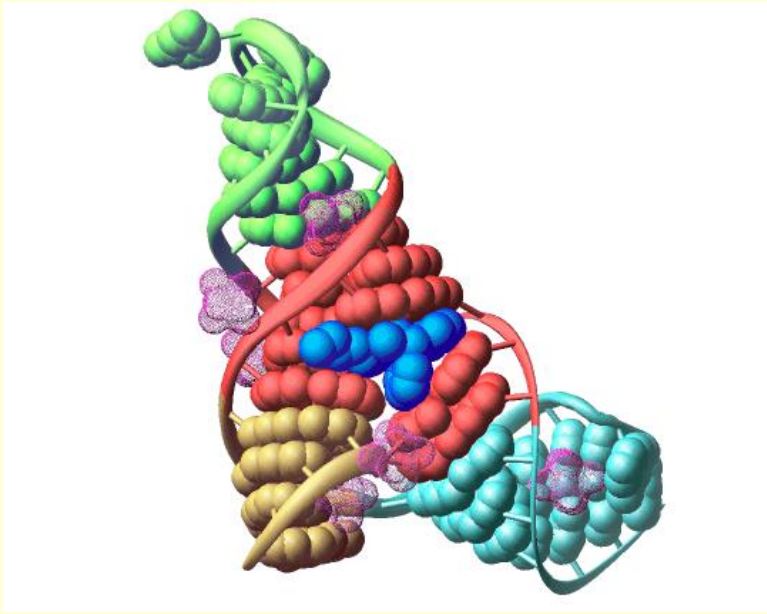

Viral suppressor of RNAi p19

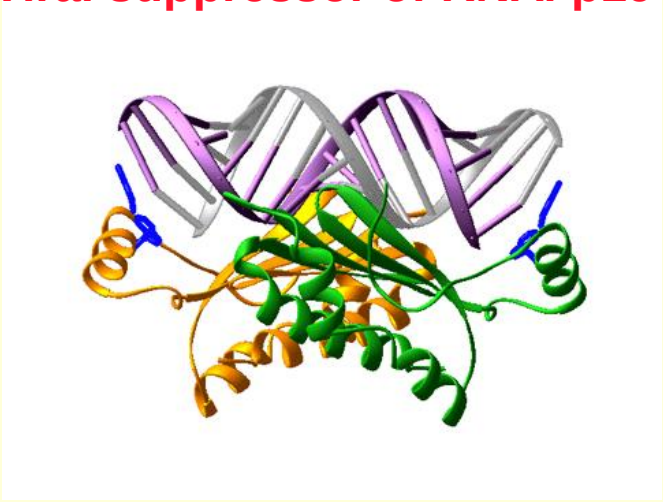

Minute Virus of Mice

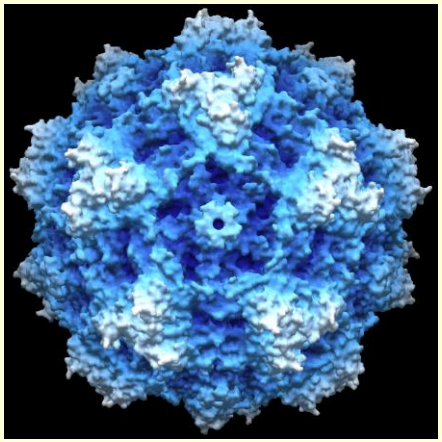

Basic techniques of STRUCTURAL BIOLOGY

•Macromolecular X-ray Crystallography	Molecules, complexes, assemblies - as single crystals
•Electron Microscopy - EM	Useful for very large assemblies, where X-ray crystallography becomes very difficult
•Nuclear Magnetic Resonance - NMR	Molecules in solution; useful to study flexible parts, invisible for X-ray crystallography

PDB

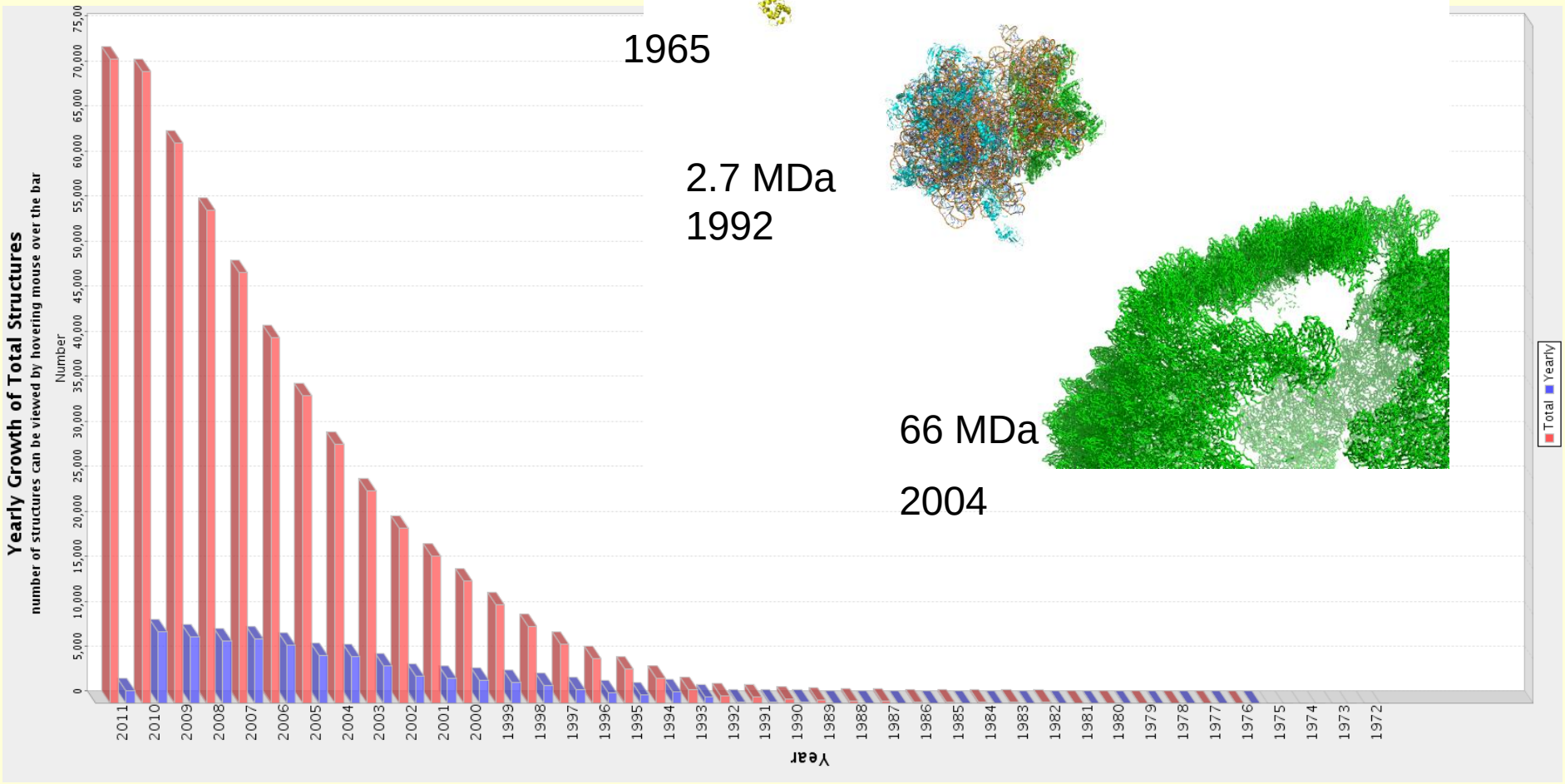
15 kDa
1965
2.7 MDa
1992
66 MDa
2004
Yearly Growth of Total Structures
number of structures can be viewed by hovering mouse over the bar
Number
Year
Total
Yearly

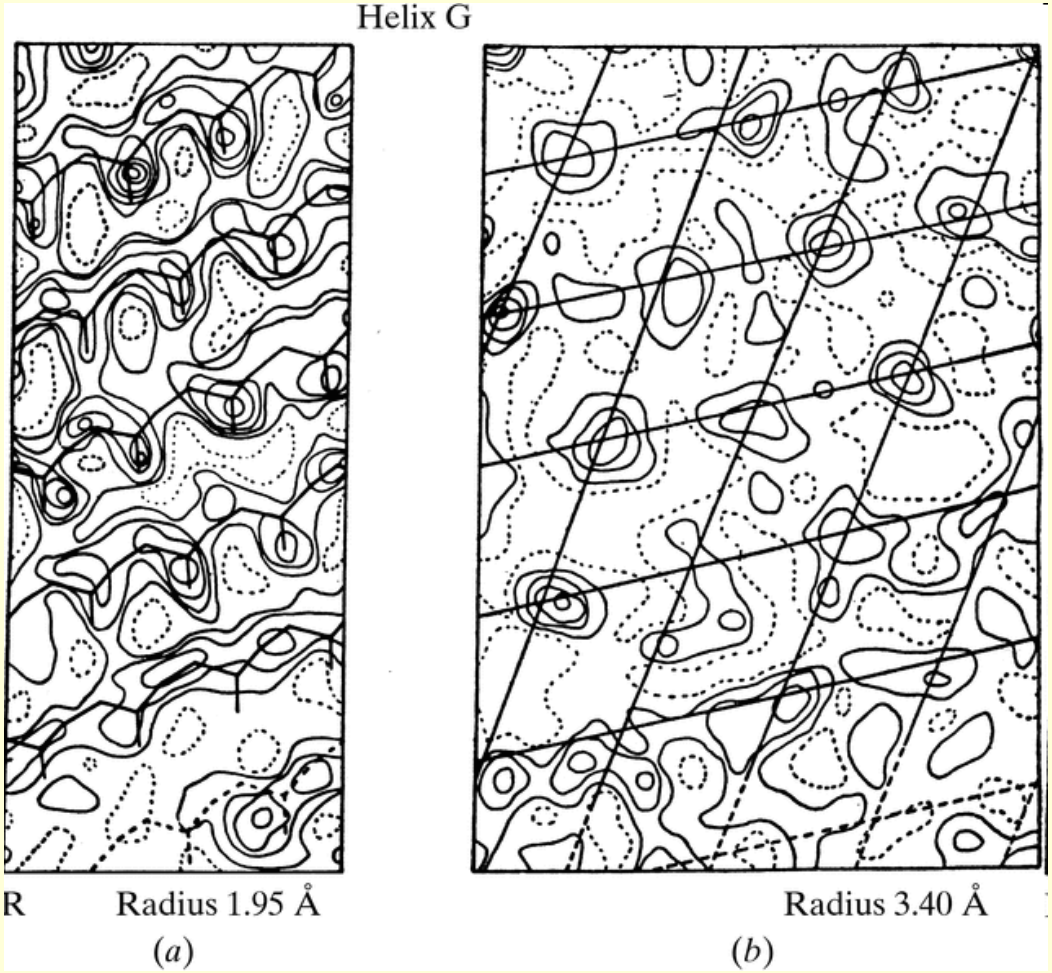

(*a*) The density in a cylindrical mantle of 1.95 Å radius, corresponding to the mean radius of the main-chain atoms in an α-helix. The calculated atomic positions of the α-helix are superimposed and roughly correspond to the density peaks. (*b*) The density at the radius of the β-carbon atoms; the positions of the β-carbon atoms calculated for a right-handed α-helix are marked by the superimposed grid (Kendrew & Watson, unpublished). Reprinted with permission from Perutz (1962). Copyright (1962) Elsevier Publishing Co.

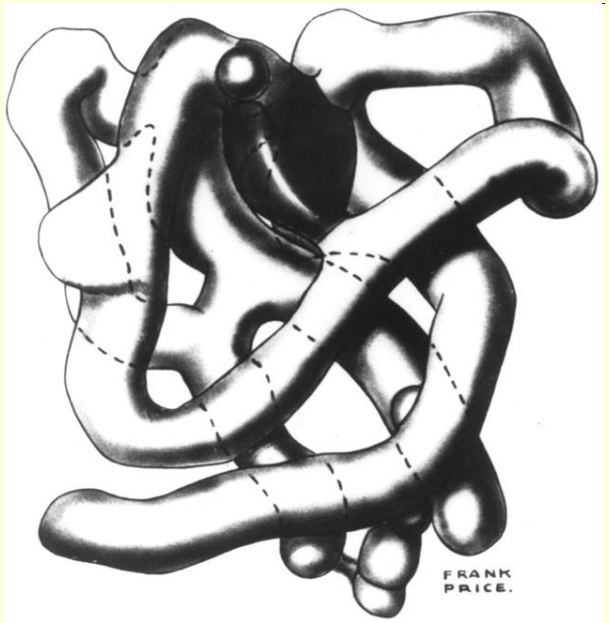

A model of the myoglobin molecule at 6 Å resolution (1959).

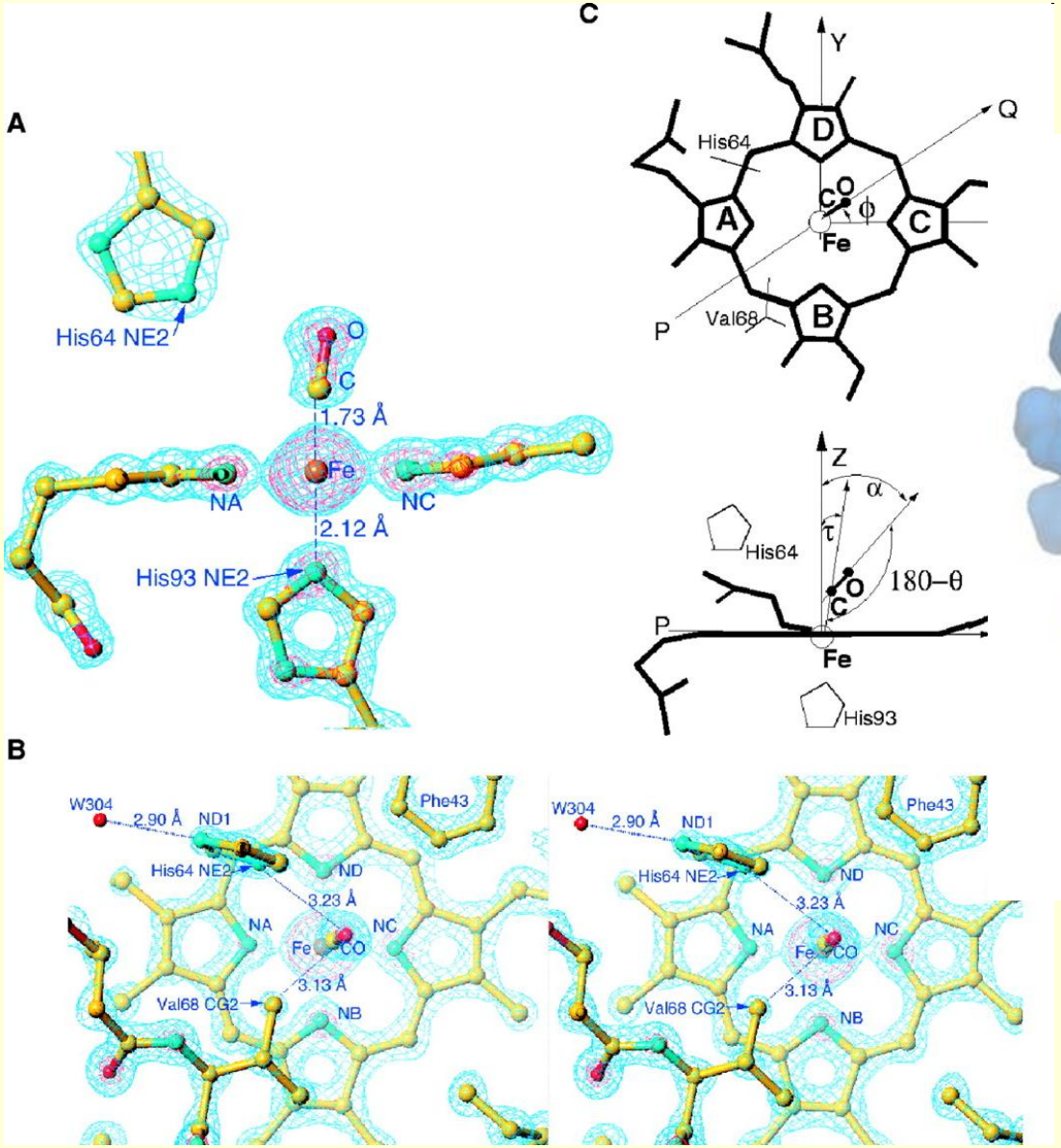

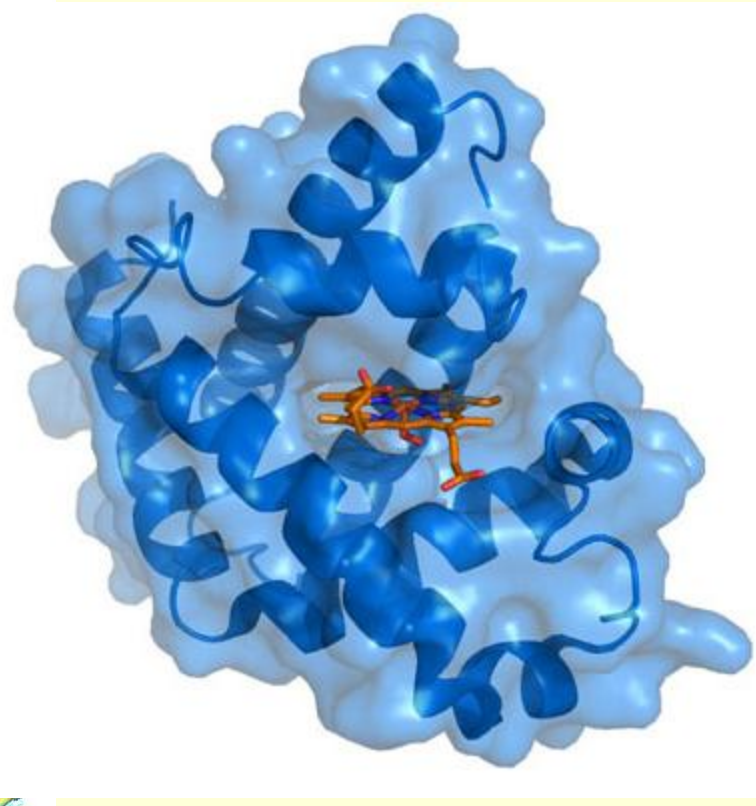

A Steric Mechanism for Inhibition of CO Binding to Heme Proteins

***Kachalova*, G. S., *Popov*, A. N. & Bartunik, H. D.. (1999). Science, 284, 473**

Proteins are formed by a chain of repeating molecules. One such molecule is called an amino-acid. There are 20 types of amino-acids but they have all a common backbone or main-chain:

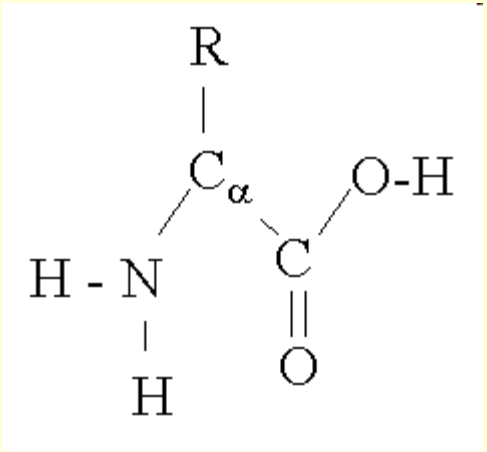

An α-amino acid.

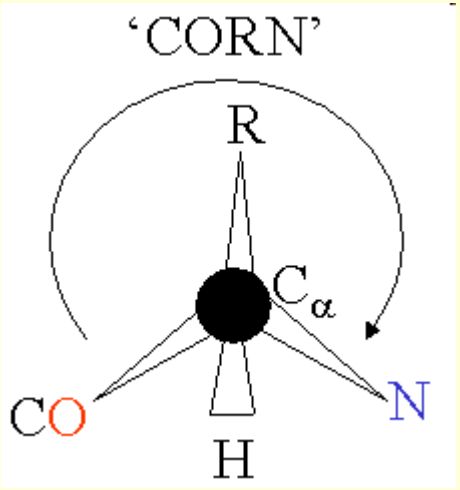

Two amino acids.

The protein chain is formed by linking the amino-acids together. The linkage is called the peptide bond:

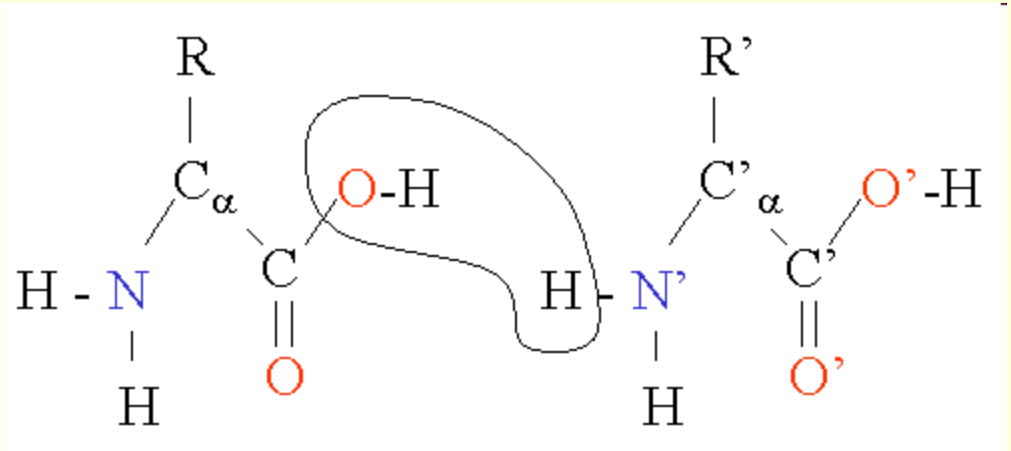

Structure in four dimensions:

Primary Structure: Amino-acid sequence.

Secondary Structure: Local regular structure: α-helices and β-sheets.

Tertiary Structure: Packing of secundary structure into one or several compact globular domains

Quarternary Structure: The arrangement of several folded chains together:multimeric proteins

Water in and around protein

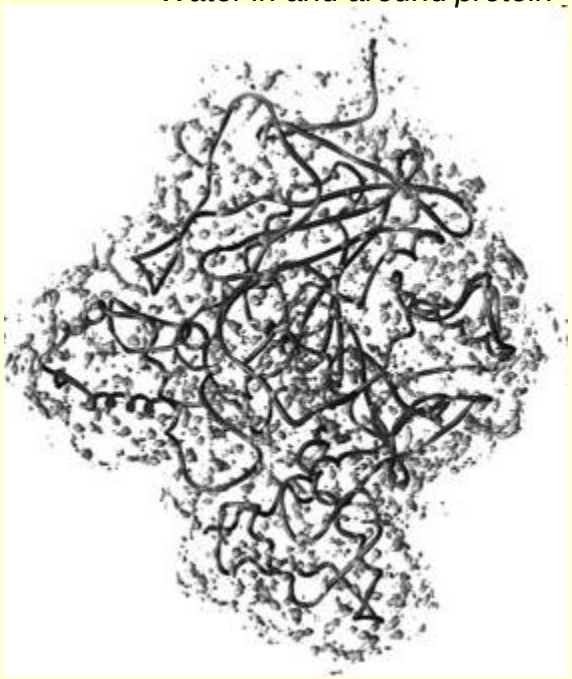

Water density isocontour for the bulk water density. AChE (actylcholine esterase) is the dark gray ribbon, oriented with the amino terminus at the *top* and carboxyl terminus at the lower *left*. In the *middle* is the active site gorge

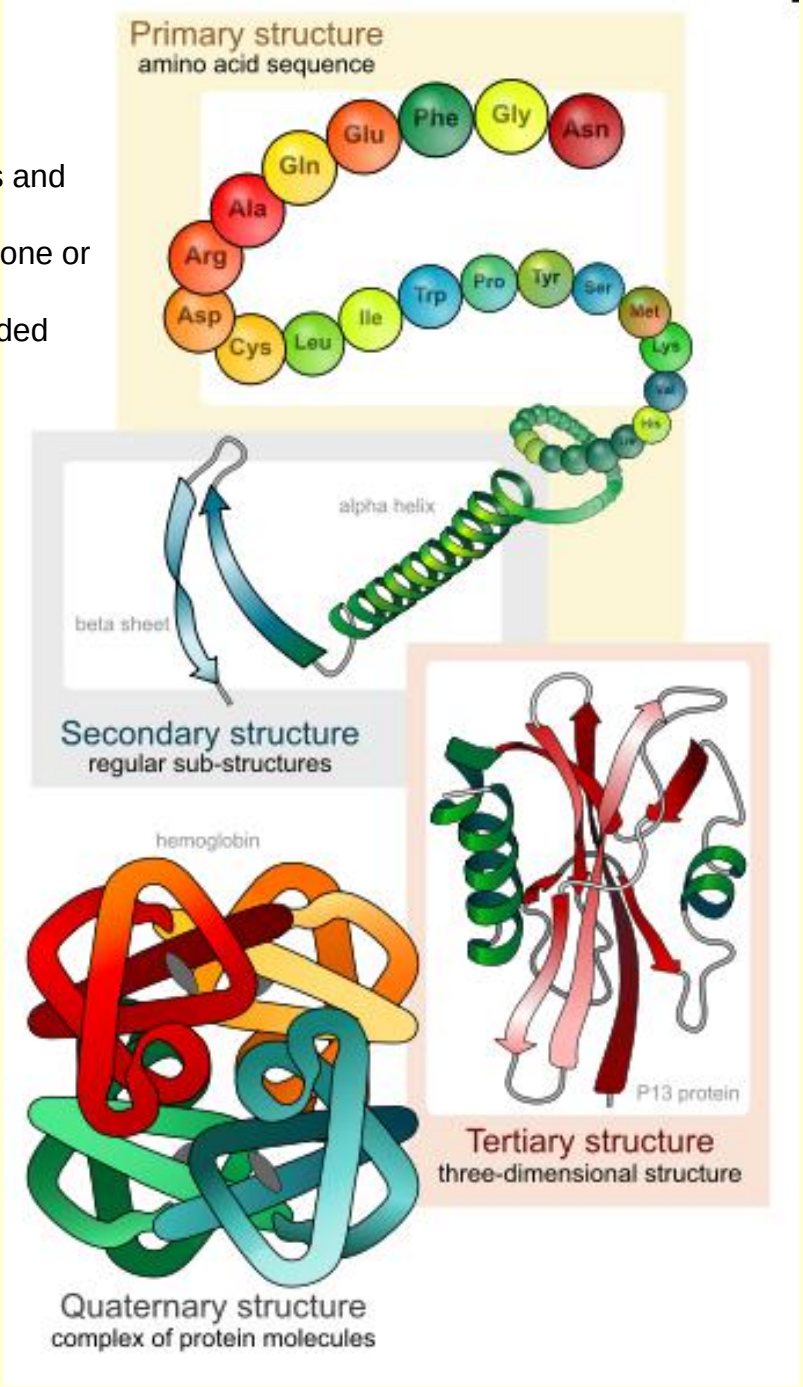

α-Helix

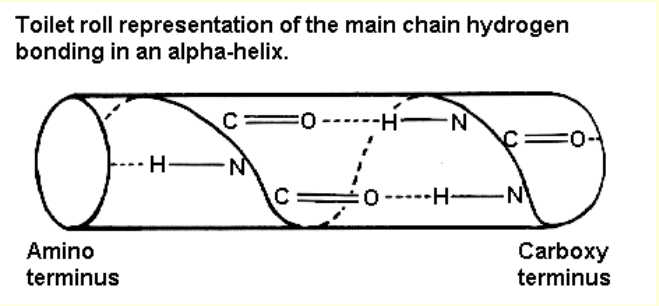

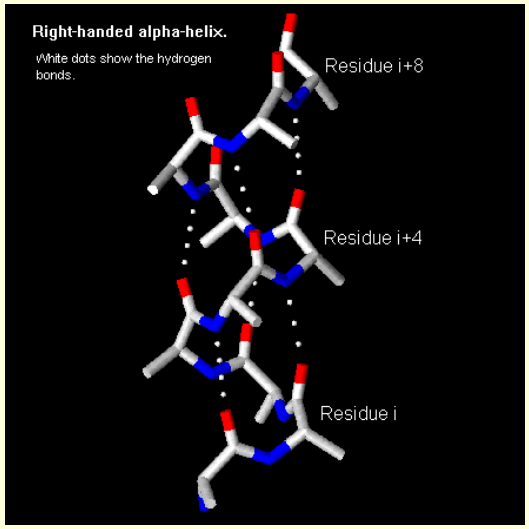

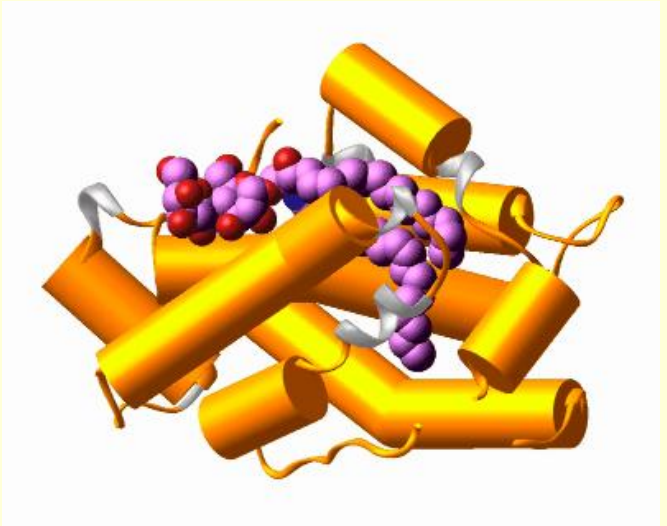

β-Structure

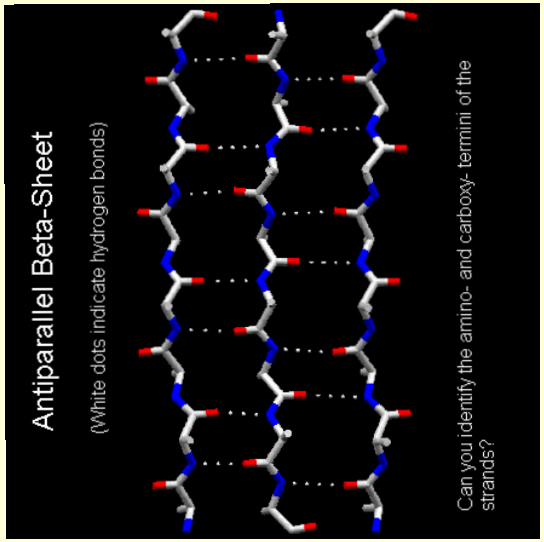

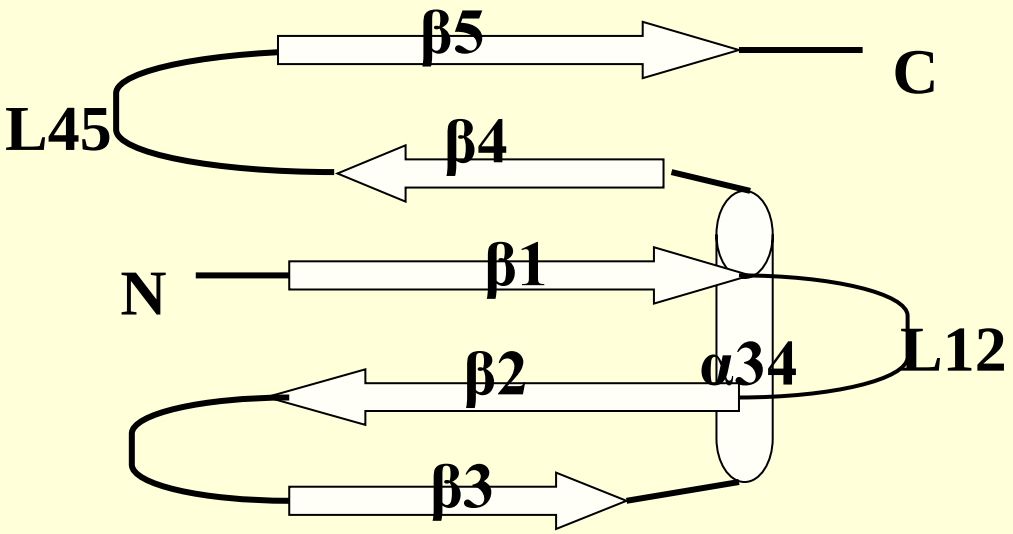

Turns

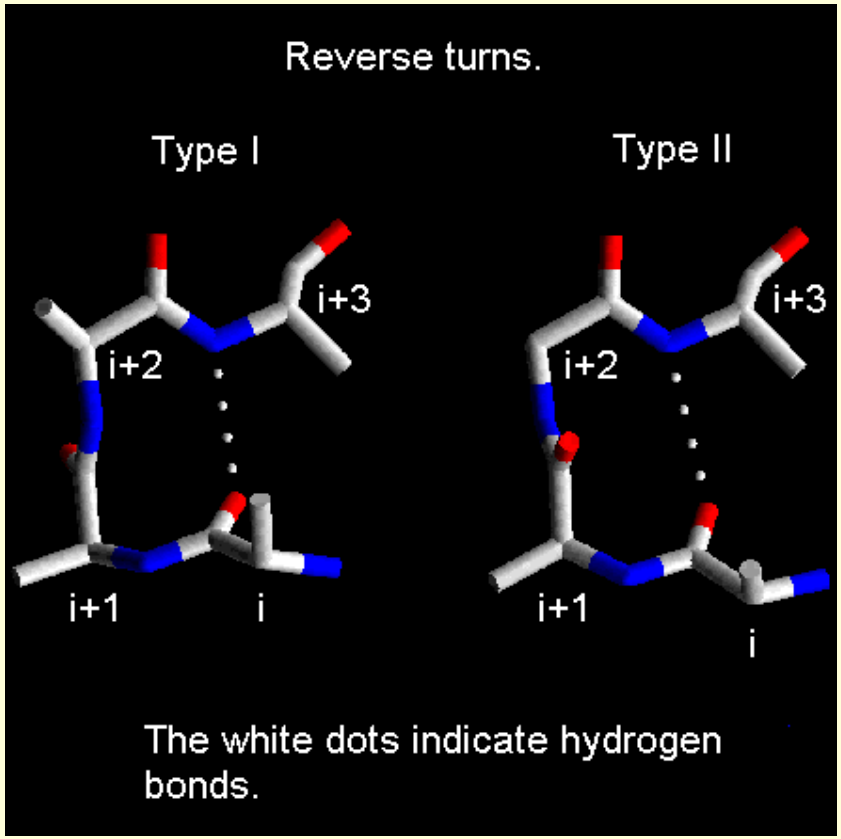
Reverse turns.
Type I
Type II
i+3
i+2
i+1
i
i+3
i+2
i+1
i
The white dots indicate hydrogen bonds.

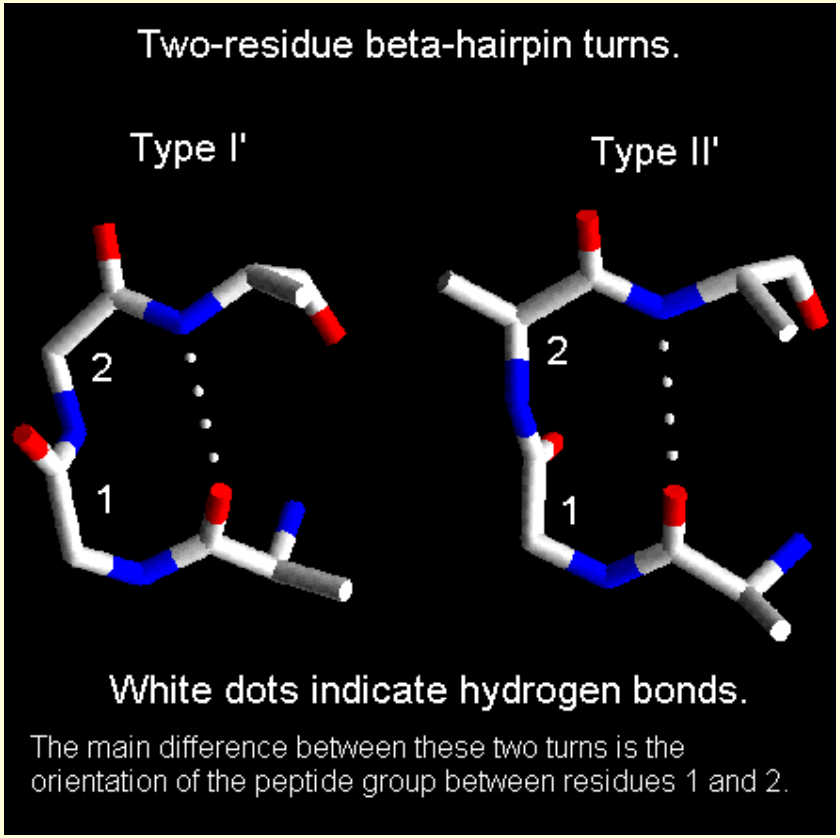
Two-residue beta-hairpin turns.
Type I'
Type II'
2
1
2
1
White dots indicate hydrogen bonds.
The main difference between these two turns is the orientation of the peptide group between residues 1 and 2.

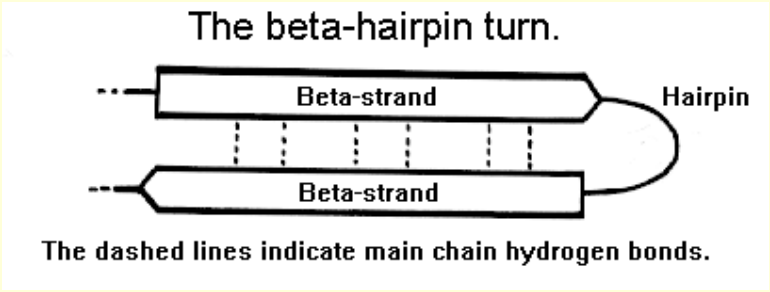
The beta-hairpin turn.
Beta-strand
Hairpin
Beta-strand
The dashed lines indicate main chain hydrogen bonds.

Why study structure?

Digestive serine proteases - Catalytic mechanism.

Hydrolysis is a chemical process in which a certain molecule is split into two parts by the addition of a molecule of water.

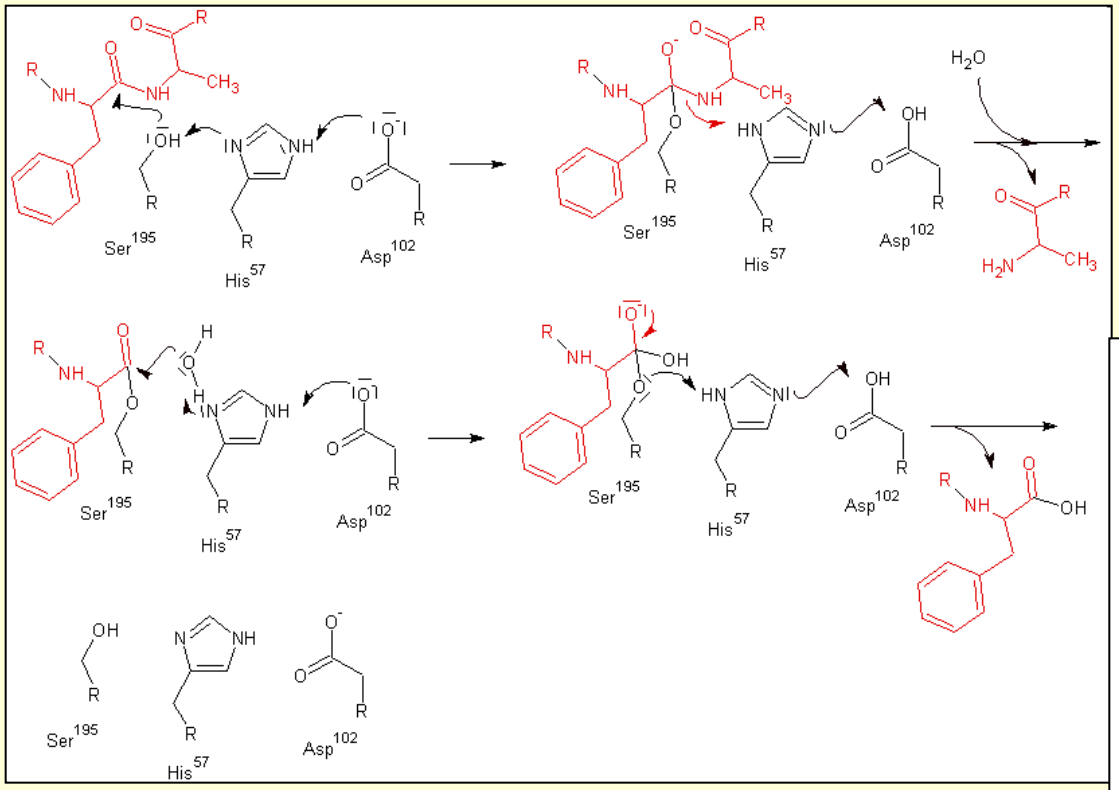

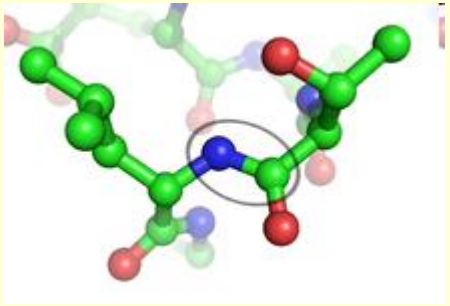

Peptide bond

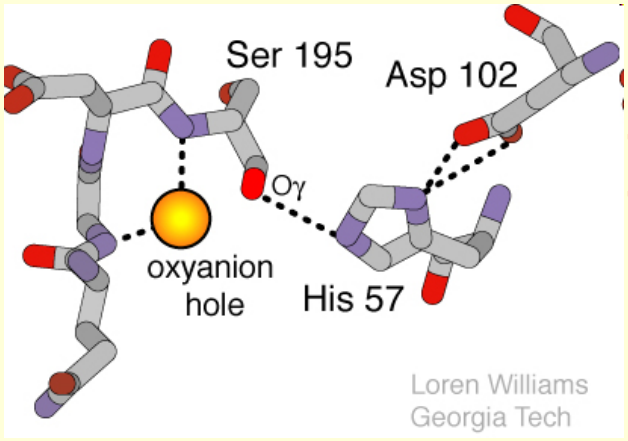

The Catalytic Triad of Trypsin

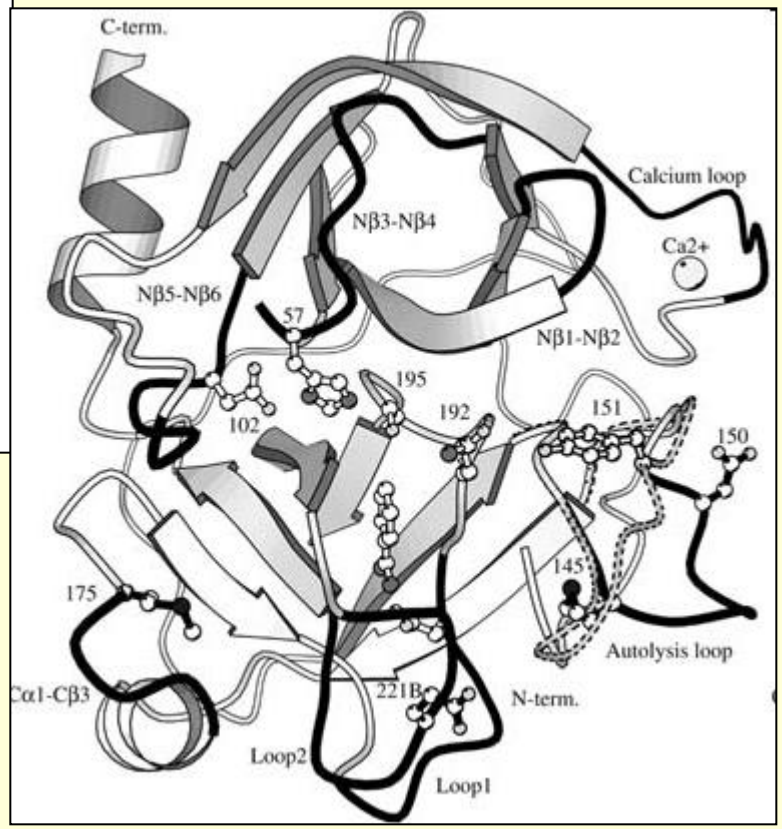

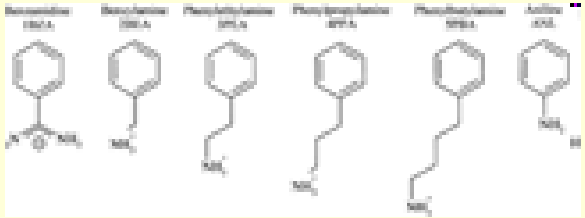

Structural formulas of the synthetic trypsin inhibitors included in the study

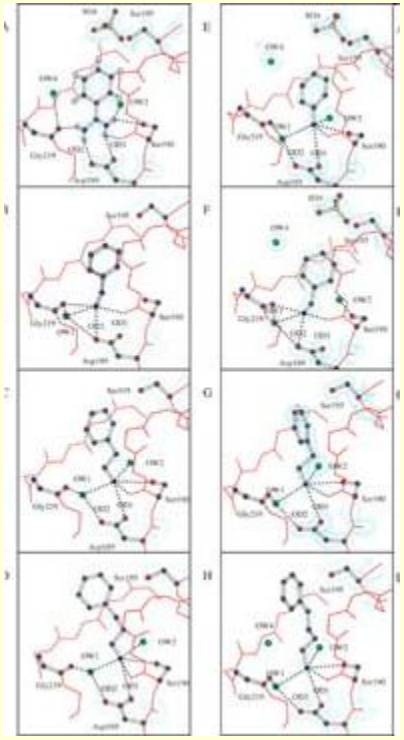

Structural arrangements, 2Fo–Fc (cyan) electron density maps and Fourier difference maps

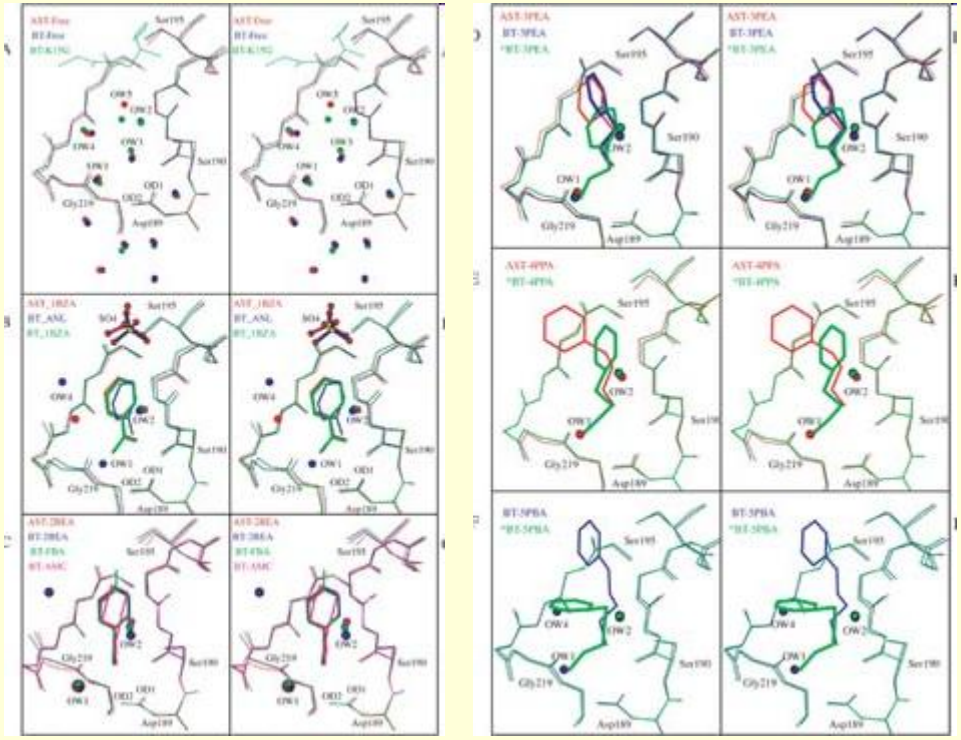

Arrangement of the superimposed S1 binding pockets and water molecules of (*A*)

Leiros at al., (April 2004). "Trypsin specificity as elucidated by LIE calculations, X-ray structures, and association constant measurements". *Protein Sci.* **13** (4): 1056–70.

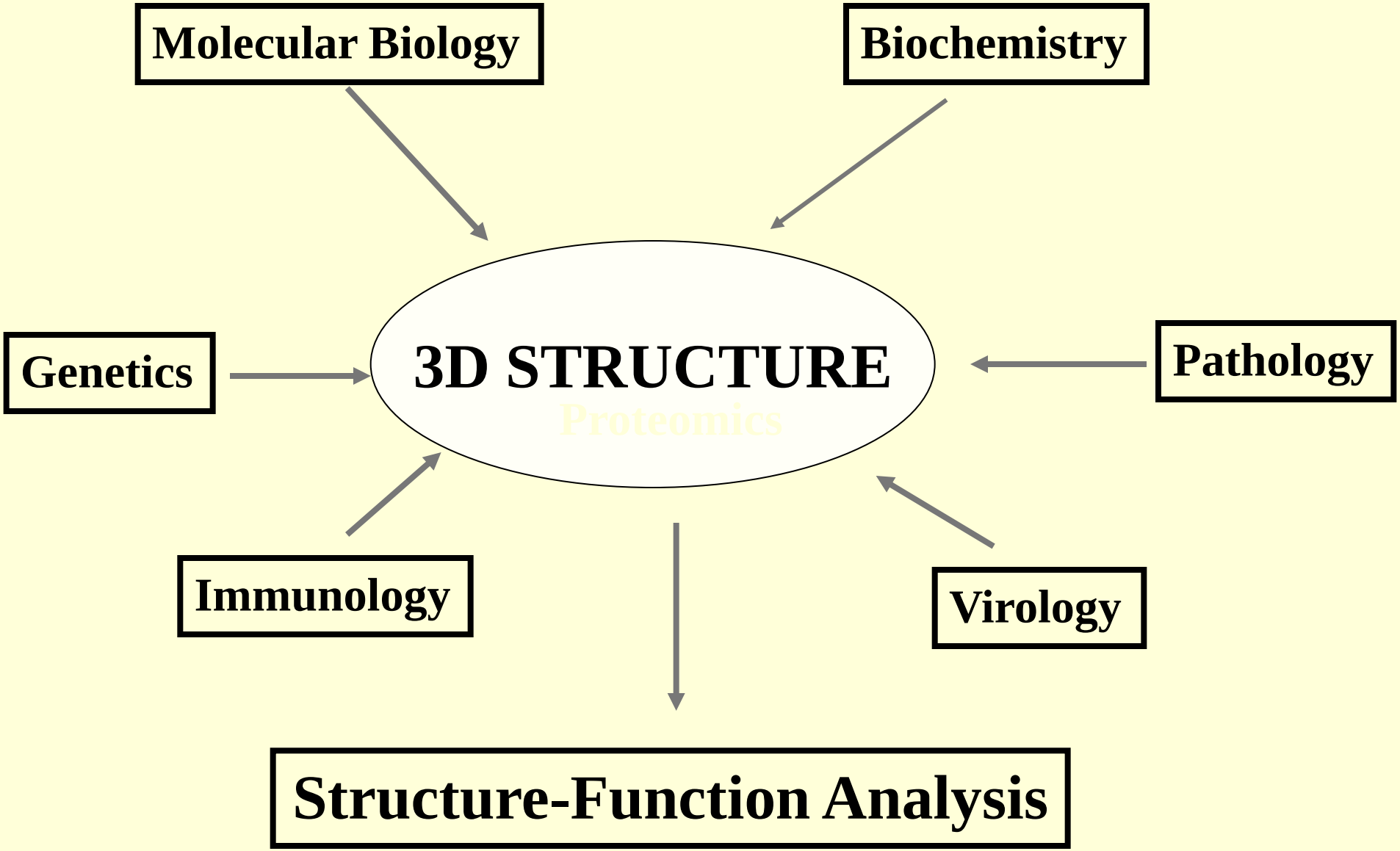
Molecular Biology
Biochemistry
Genetics
3D STRUCTURE
Proteomics
Pathology
Immunology
Virology
Structure-Function Analysis

PROSEDURE

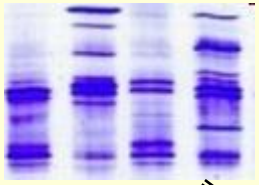

Clone gene
expressing
purification

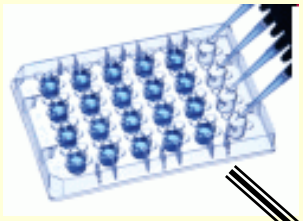

crystallization

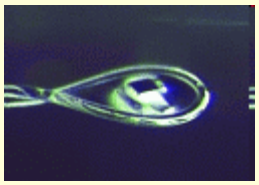

Crystal mounting

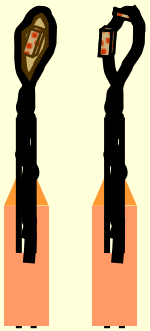

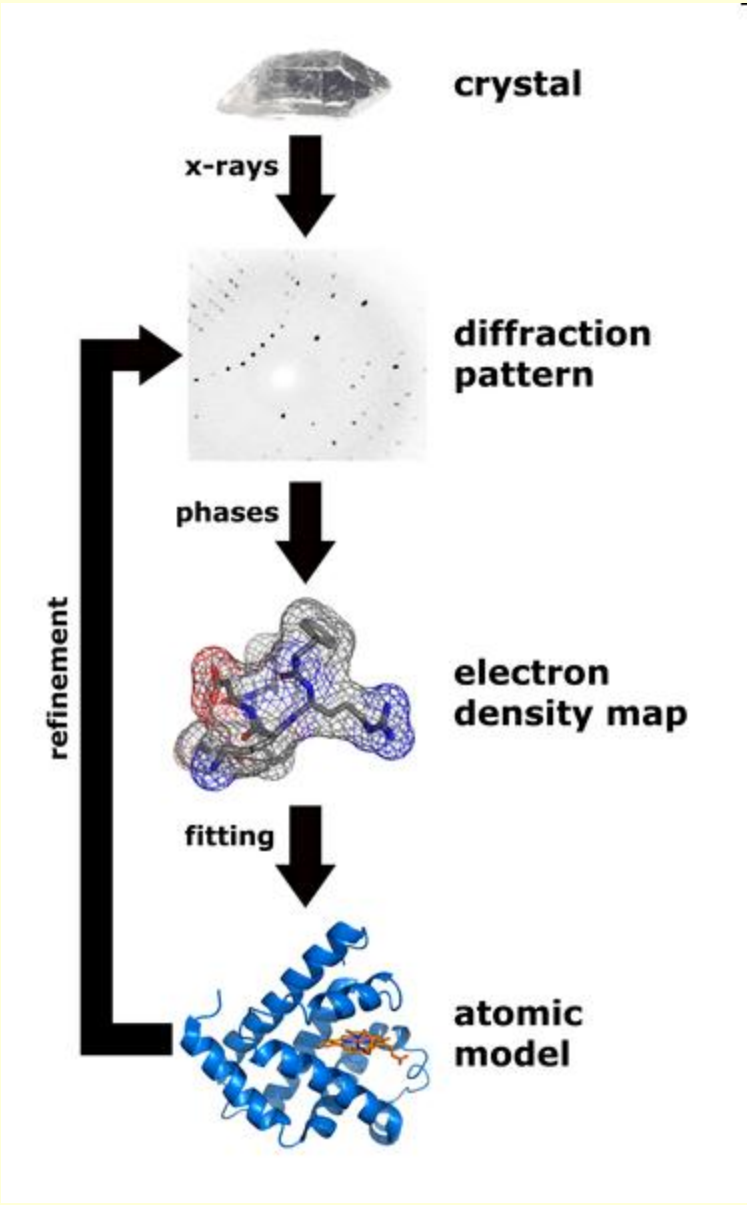

The Crystallization Experiment

Crystal Screen Kit

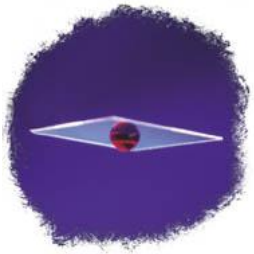

Hanging drop

Growth Techniques

1- Hanging Drop
2- Sitting Drop
3- Sandwich Drop
4- Free interface diffusion (NASA)
5- Batch (Robots)
6- Microbatch - under oil.
7- Mcrodialysis (Buttons)

Micro-bridges
(Sitting drop)

Dialysis Buttons

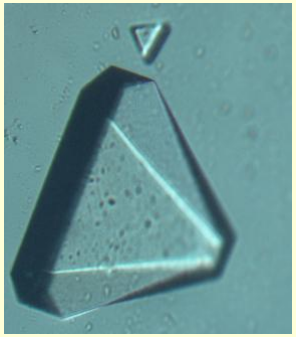

Virus Crystal
~0.15mm

$$F_{(h,k,l)} = \sum_{j=1}^{atoms} f_{(j)} \exp\left[2\pi \cdot i(hx_{(j)} + ky_{(j)} + lz_{(j)})\right]$$

$$\rho_{(x,y,z)} = \frac{1}{V} \sum_{h} \sum_{k} \sum_{l} F_{(h,k,l)} \exp\left[-2\pi \cdot i(hx + ky + lz)\right]$$

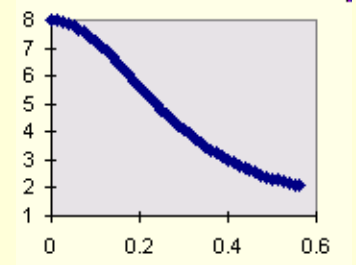

$$f^{o}(\sin\theta/\lambda) = \sum_{i=1}^{4} a_i \cdot e^{-b_i(\sin\theta/\lambda)^2} + c$$

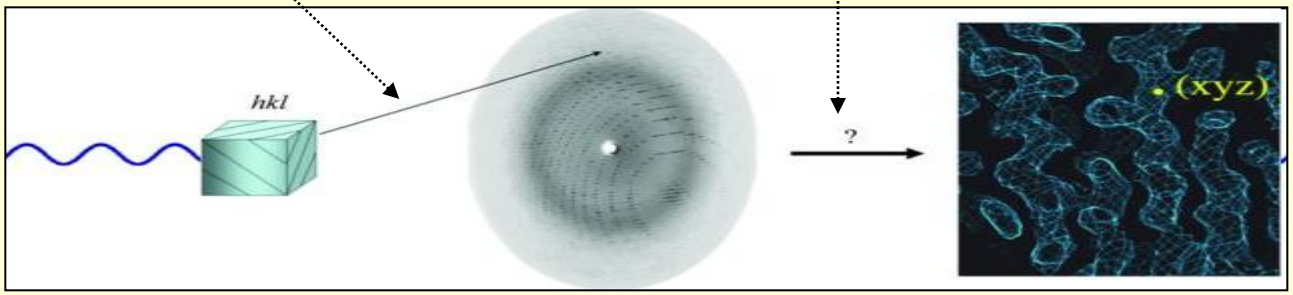

The importance of phases in carrying information. Top, the diffraction pattern, or Fourier transform (FT), of a duck and of a cat. Bottom left, a diffraction pattern derived by combining the amplitudes from the duck diffraction pattern with the phases from the cat diffraction pattern. Bottom right, the image that would give rise to this hybrid diffraction pattern. In the diffraction pattern, different colours show different phases and the brightness of the colour indicates the amplitude. Reproduced courtesy of Kevin Cowtan

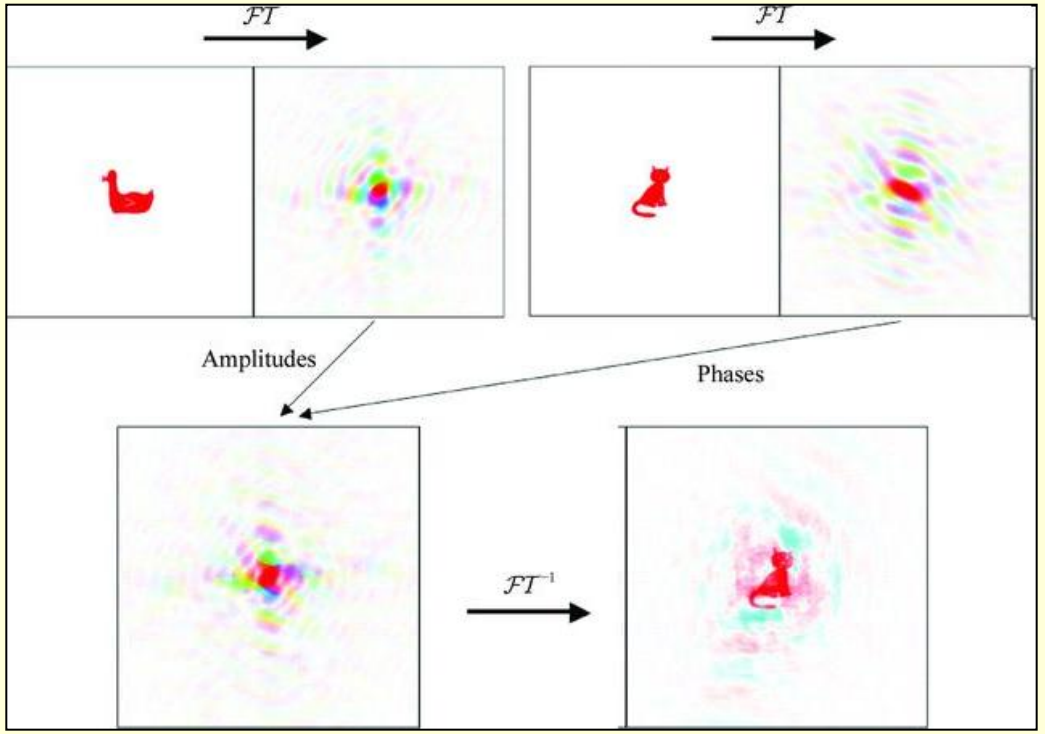

***from G.Taylor, Acta Cryst.* (2010). D66, 325-338**

The process of molecular replacement.

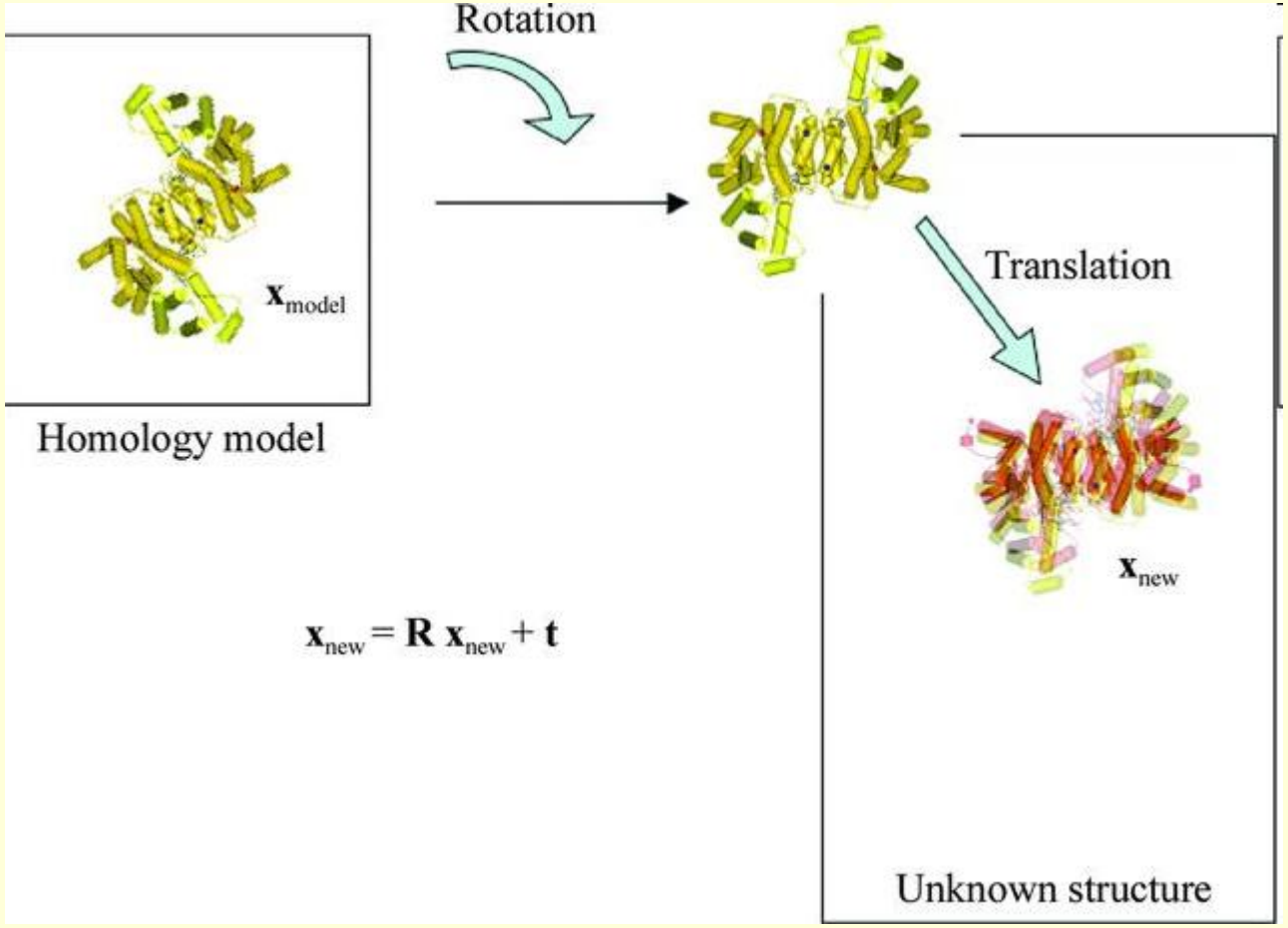

from G.Taylor, Acta Cryst. **(2010). D66, 325-338**

Isomorphous replacement

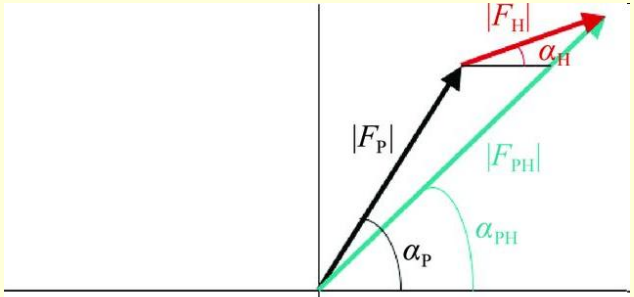

Argand diagram for SIR. |*F*P| is the amplitude of a reflection for the native crystal and |*F*PH| is that for the derivative crystal.

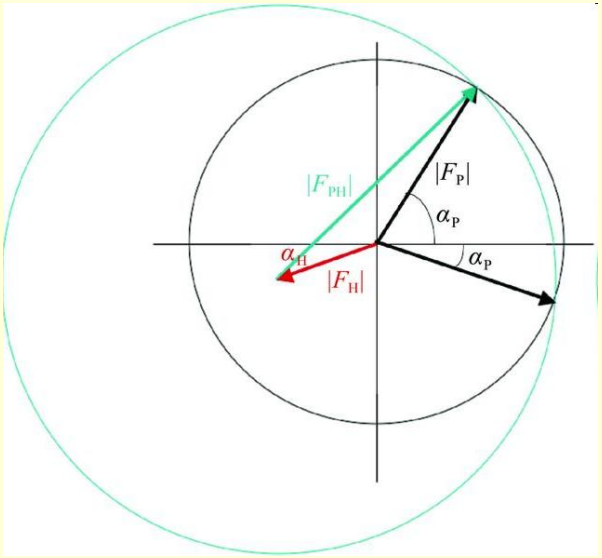

Harker construction for SIR.

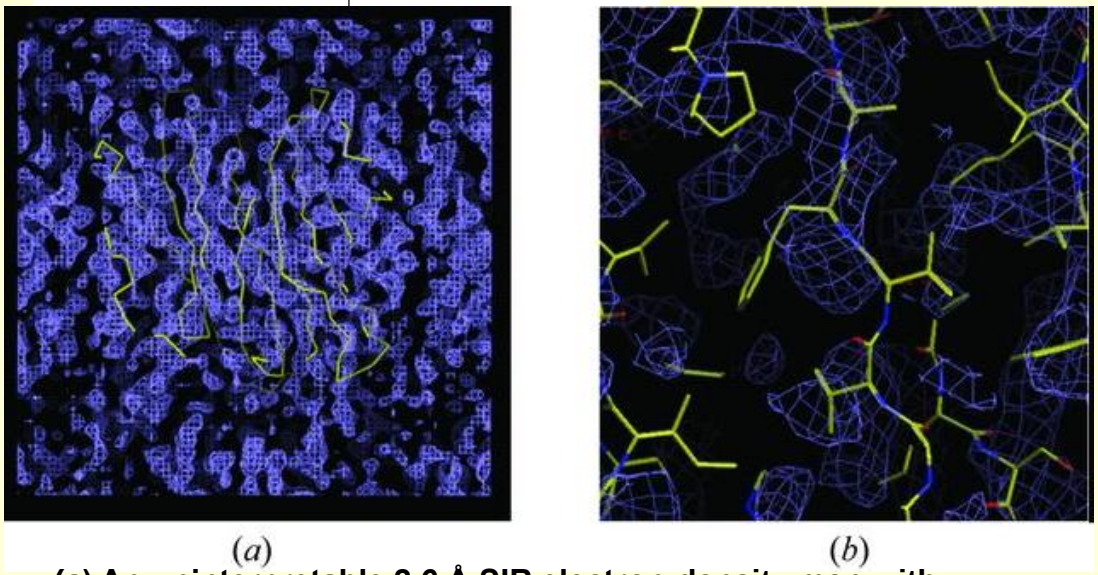

(*a*) An uninterpretable 2.6 Å SIR electron-density map with the final C trace of the structure superimposed. (x) = (1/*V*) *m*|*F*P|exp(*i* best)× exp(-2 *i*h·x). (*b*) A small section of the map with the final structure superimposed.

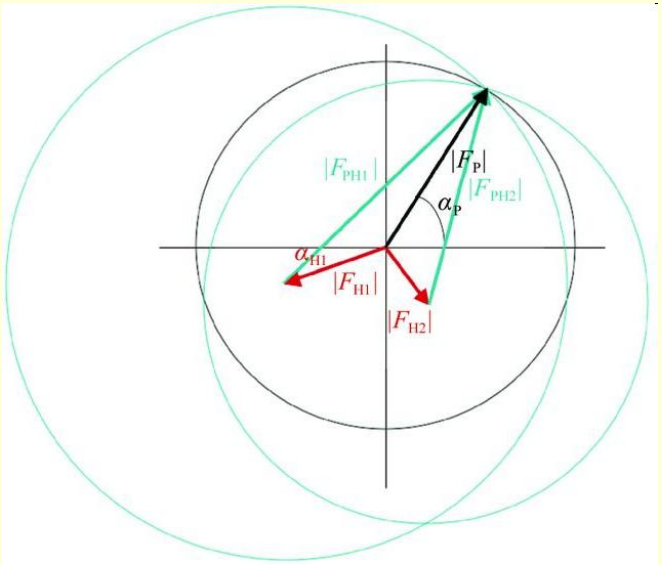

Harker diagram for MIR with two heavy-atom derivatives.

***from G.Taylor, Acta Cryst.* (2010). D66, 325-338**

Anomalous scattering

The atomic scattering factor contains three components: a normal scattering term *f*0 that is dependent on the Bragg angle and two terms *f'* and *f''* that are not dependent on scattering angle but are dependent on scattering angle.

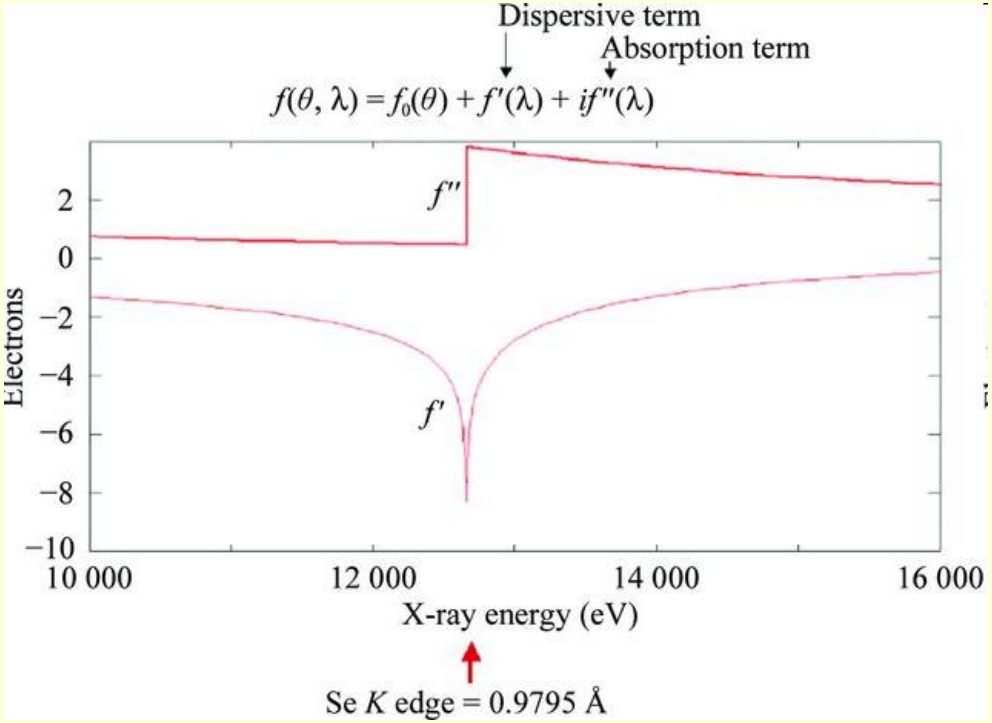

Variation in anomalous scattering signal *versus* incident X-ray energy in the vicinity of the *K* edge of selenium

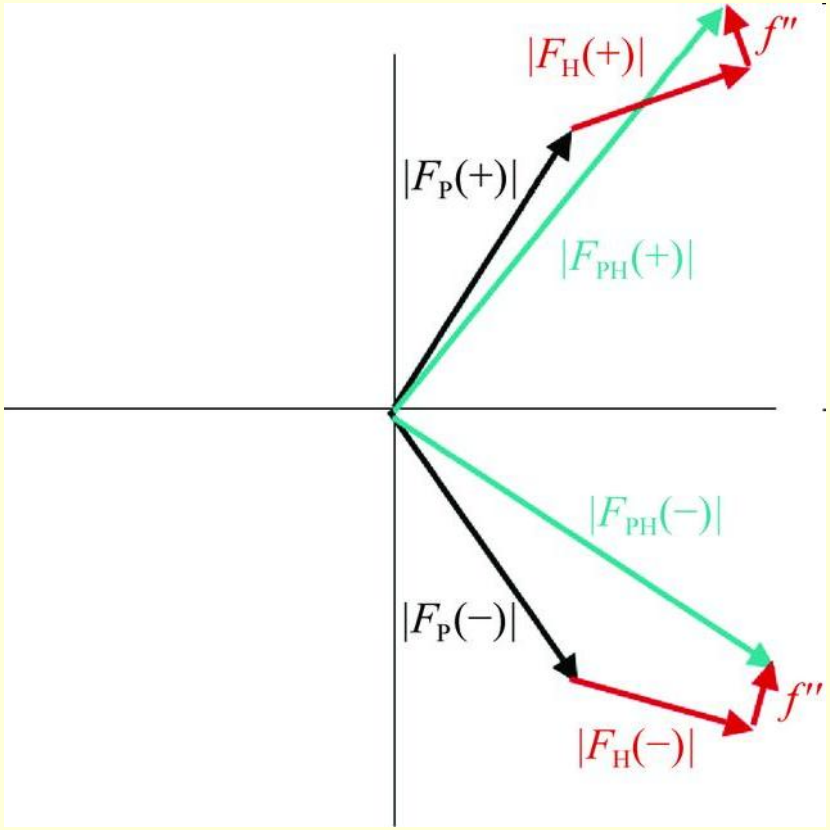

Breakdown of Friedel's law when an anomalous scatterer is present. *f*(,) = *f*0( ) + *f'*( ) + *if''*( ). |*Fhkl*| |*F-h-k-l*| or |*F*PH(+)| |*F*PH(-)|. *F*± = |*F*PH(+)| - |FPH(-)| is the Bijvoet difference.

***from G.Taylor, Acta Cryst.* (2010). D66, 325-338**

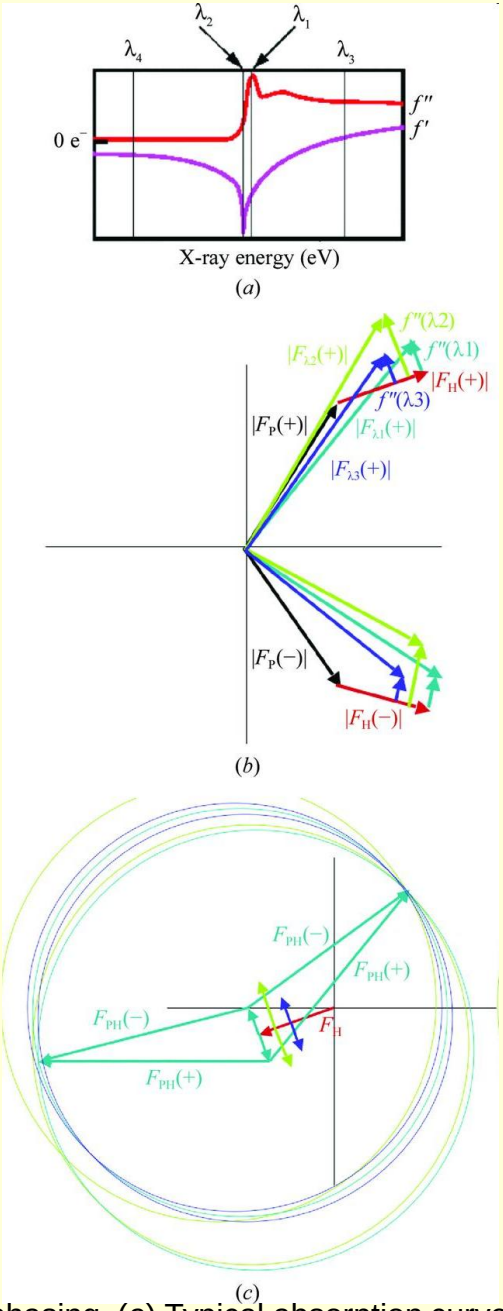

MAD phasing. (*a*) Typical absorption curve for an anomalous scatterer. (*b*) Phase diagram. |*F*P| is not measured, so one of the data sets is chosen as the `native'. (*c*) Harker construction.

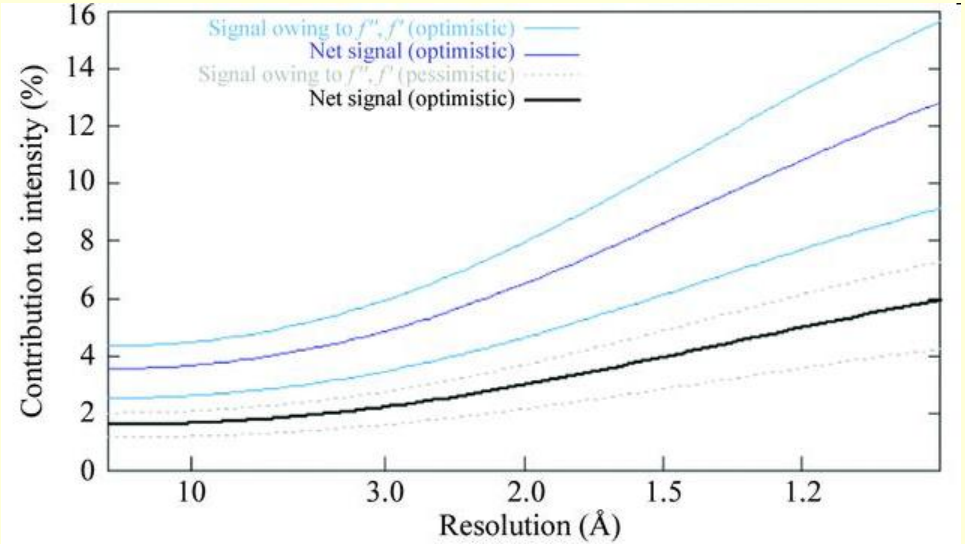

Estimation of signal size. The expected Bijvoet ratio is r.m.s.(*F*±)/r.m.s.(|*F*|) (*N*A/2*N*T)1/2(2*f*''A/*Z*eff). The expected dispersive ratio is r.m.s.(*F*)/r.m.s.(|*F*|) (*N*A/2*N*T)1/2[|*f*'A(*i*) - *f*'A(*j*)|]/*Z*eff, where *N*A is the number of anomalous scatterers, *N*T is the total number of atoms in the structure and *Z*eff is the normal scattering power for all atoms (6.7 e- at 2 = 0)

***from G.Taylor, Acta Cryst.* (2010). D66, 325-338**

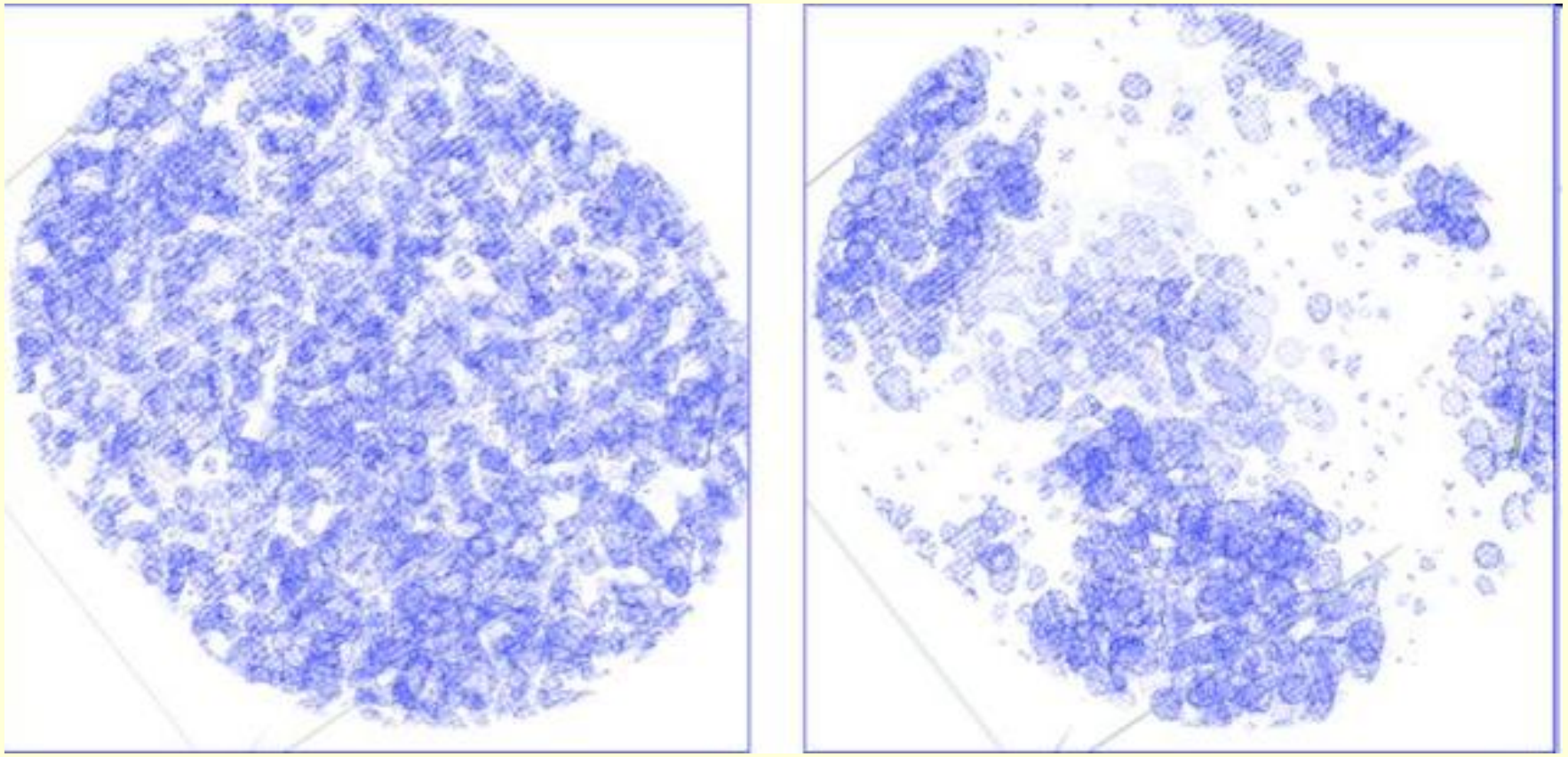

2.1 Å electron-density map for the S-SAD example before and after density modification using *SHELXE*.

***from G.Taylor, Acta Cryst.* (2010). D66, 325-338**

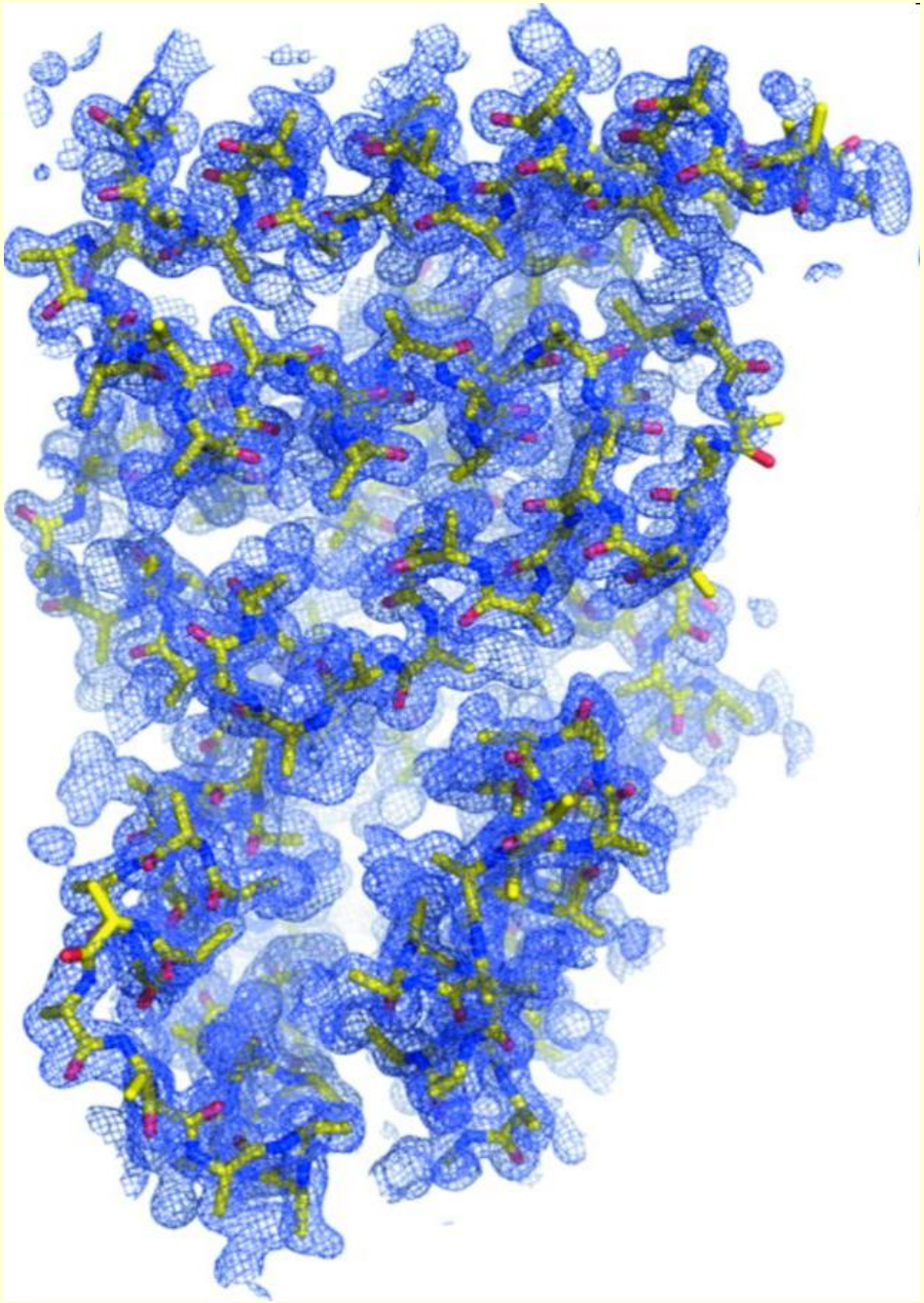

Autotraced polyalanine model produced by *SHELXE* superimposed on the density-modified electron-density map at 1.45 Å resolution.

***from G.Taylor, Acta Cryst.* (2010). D66, 325-338**

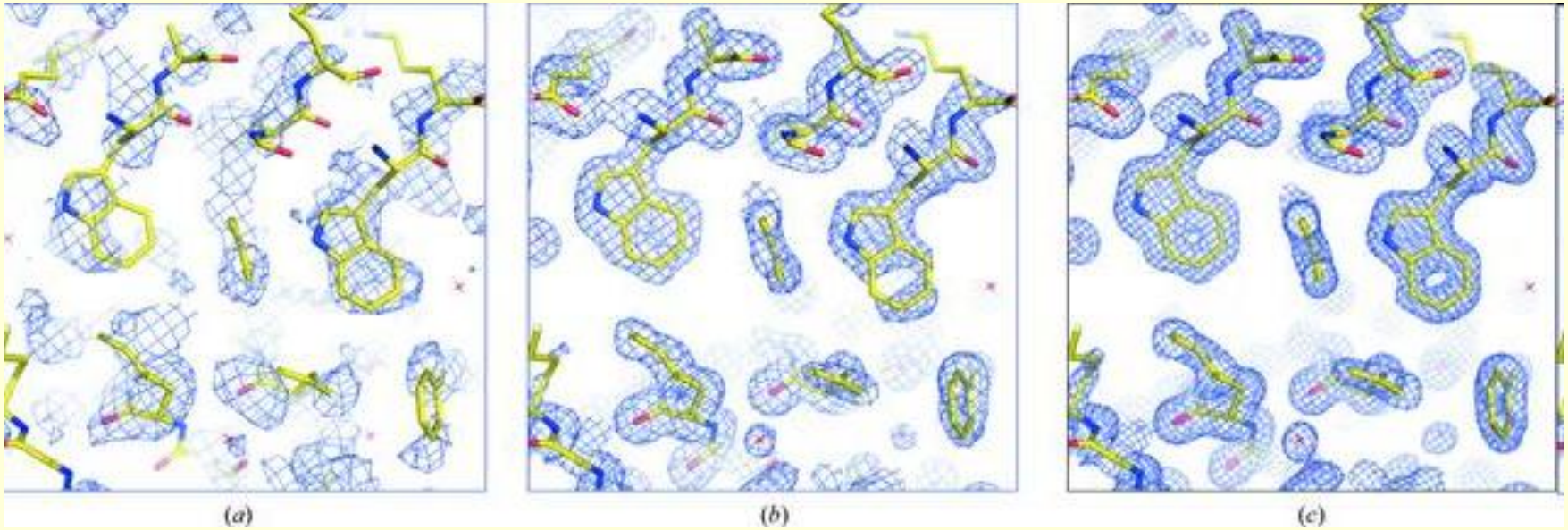

Improving phases for the S-SAD problem. (*a*) 2.1 Å resolution density-modified map. (*b*) 1.45 Å resolution phase-extended map. (*c*) `1.0 Å resolution' free-lunch map

***from G.Taylor, Acta Cryst.* (2010). D66, 325-338**

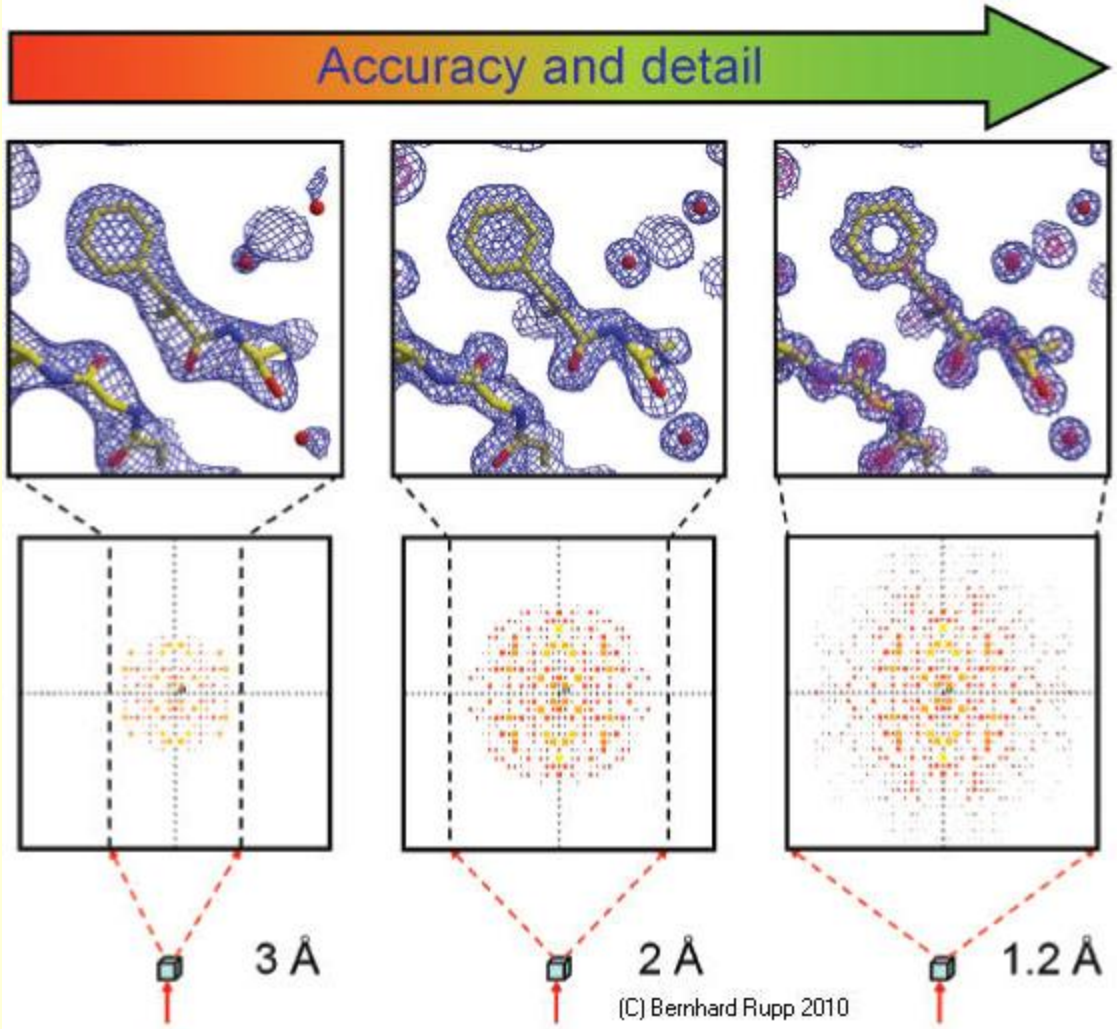

Figure 1-6 Data quality determines structural detail and accuracy. The qualitative relation between the extent of X-ray diffraction, the resulting amount of available diffraction data, and the quality and detail of the electron density reconstruction and protein structure model are evident from this figure: The crystals are labeled with the nominal resolution d_{min} given in Å (Ångström) and determined by the highest diffraction angle (corresponding to the closest sampling distance in the crystal, thus termed d_{min}) at which X-ray reflections are observed. Above each crystal is a sketch of the corresponding diffraction pattern, which contains significantly more data at higher resolution, corresponding to a smaller distance between discernible objects of approximately d_{min}. As a consequence, both the reconstruction of the electron density (blue grid) and the resulting structure model (stick model) are much more detailed and accurate. The non-SI unit Å (10^{-8} cm or 0.1 nm = 10^{-10} m) is frequently used in the crystallographic literature, simply because it is of the same order of magnitude as atomic radii (~0.77 Å for carbon) or bond lengths (~1.54 Å for the C–C single bond).

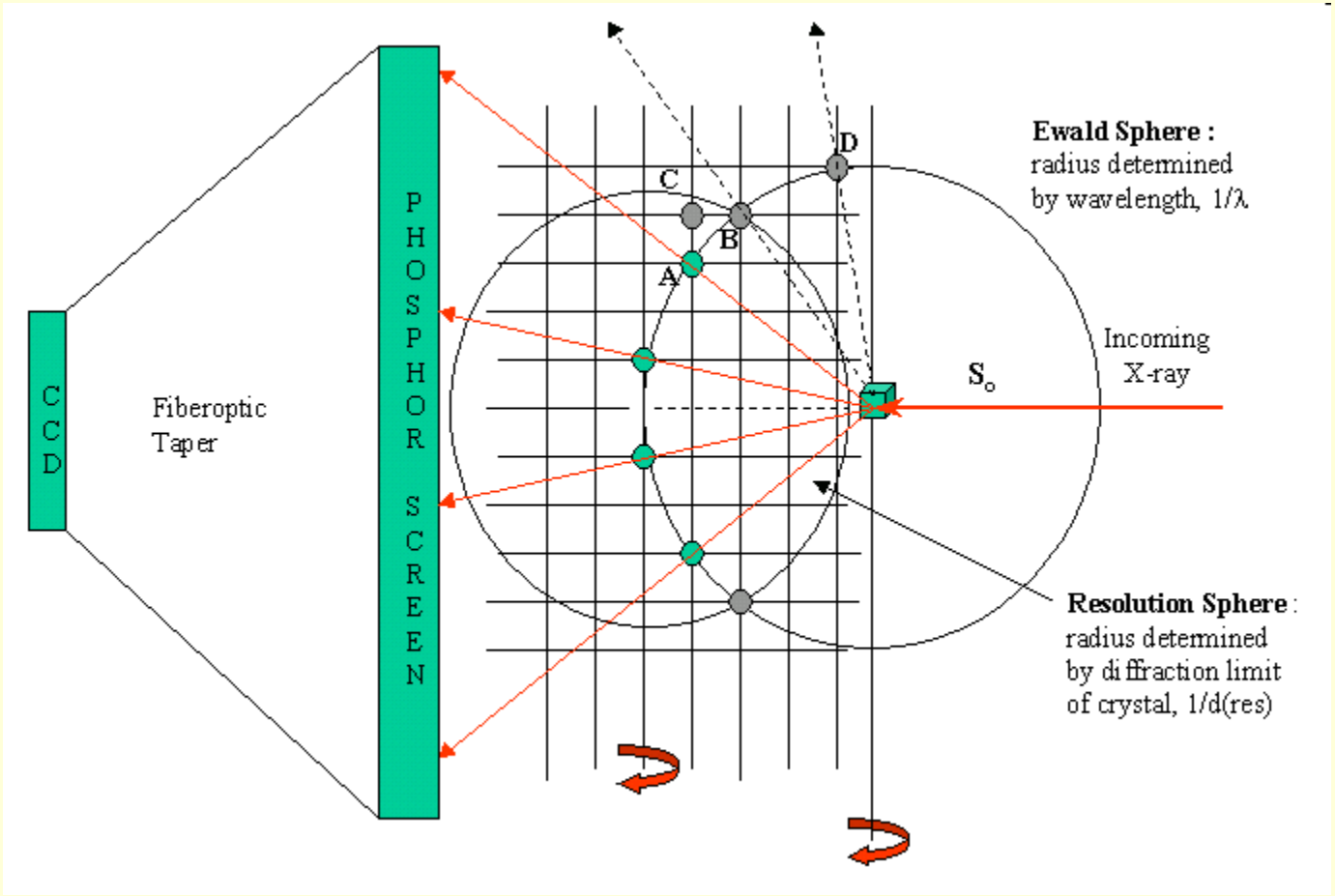
CCD
Fiberoptic
Taper
PHOSPHOR SCREEN
A
B
C
D
Ewald Sphere :
radius determined
by wavelength, 1/λ
Incoming
X-ray
S0
Resolution Sphere :
radius determined
by diffraction limit
of crystal, 1/d(res)

Darwin's Formula

$$I(hkl) = I_{beam}\, r_e^2\, \frac{V_{xtal}}{V_{cell}}\, \frac{\lambda^3 L}{\omega V_{cell}}\, P\, A\, |\, F(hkl)\, |^2$$

I(hkl) - photons/spot (fully-recorded)

I_{beam} - incident (photons/s/m^2)

r_e - classical electron radius (2.818×10^{-15} m)

V_{xtal} - volume of crystal (in m^3)

V_{cell} - volume of unit cell (in m^3)

λ - x-ray wavelength (in meters!)

ω - rotation speed (radians/s)

L - Lorentz factor (speed/speed)

P - polarization factor

$(1+\cos^2(2\theta) - Pfac \cdot \cos(2\Phi)\sin^2(2\theta))/2$

A - absorption factor

$\exp(-\mu_{xtal} \cdot l_{path})$

F(hkl) - structure amplitude (electrons)

C. G. Darwin (1914)

Complications 1

Large cell parameters

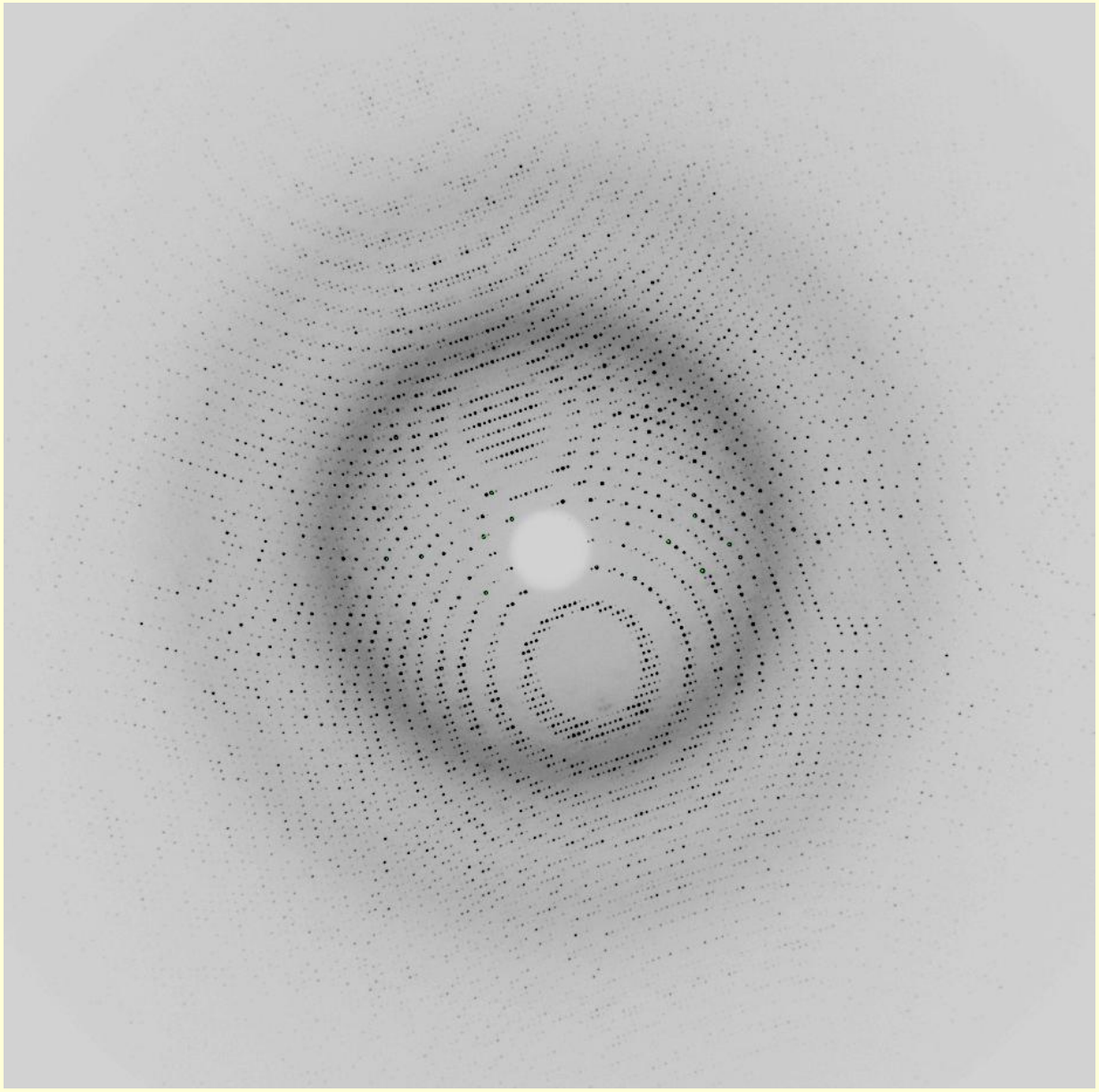

Complications 2

- **Weak diffraction intensity – light atoms**
- **Poor crystal quality – big B-factor**
- **Background intensity > diffraction intensity**

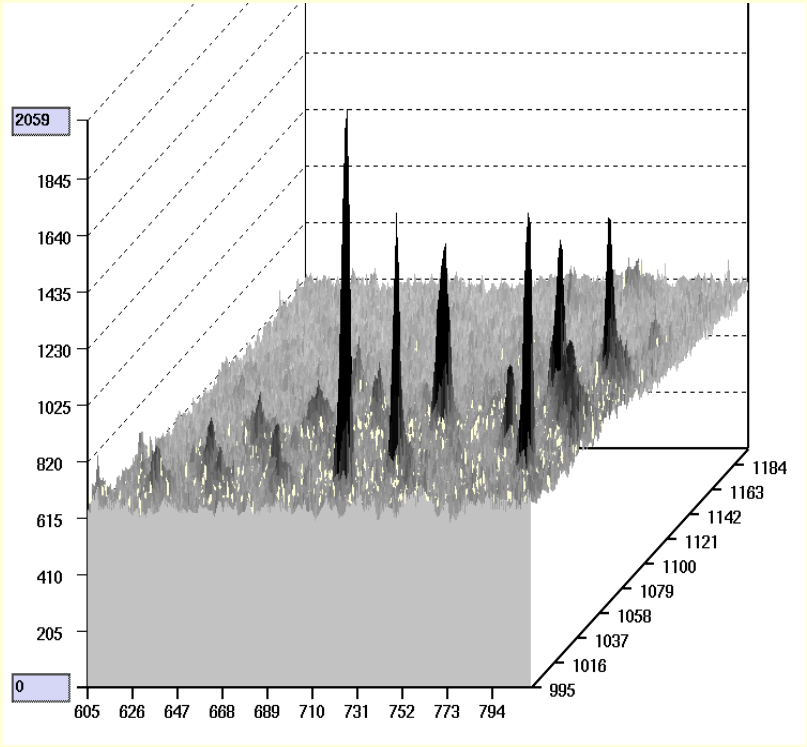

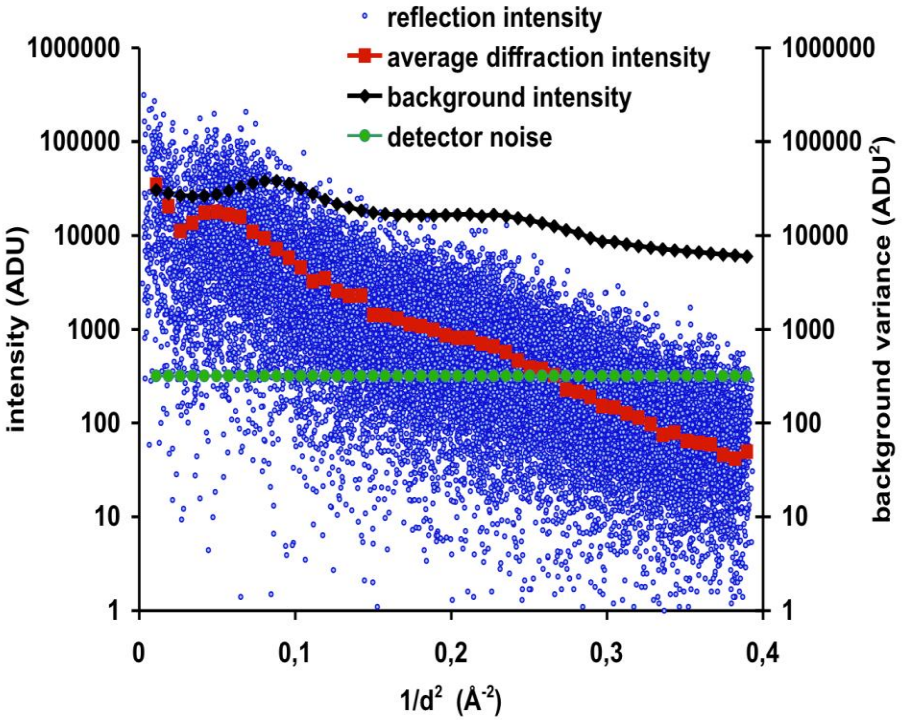

Complications 3
Radiation damage

Photon interaction with soft matter

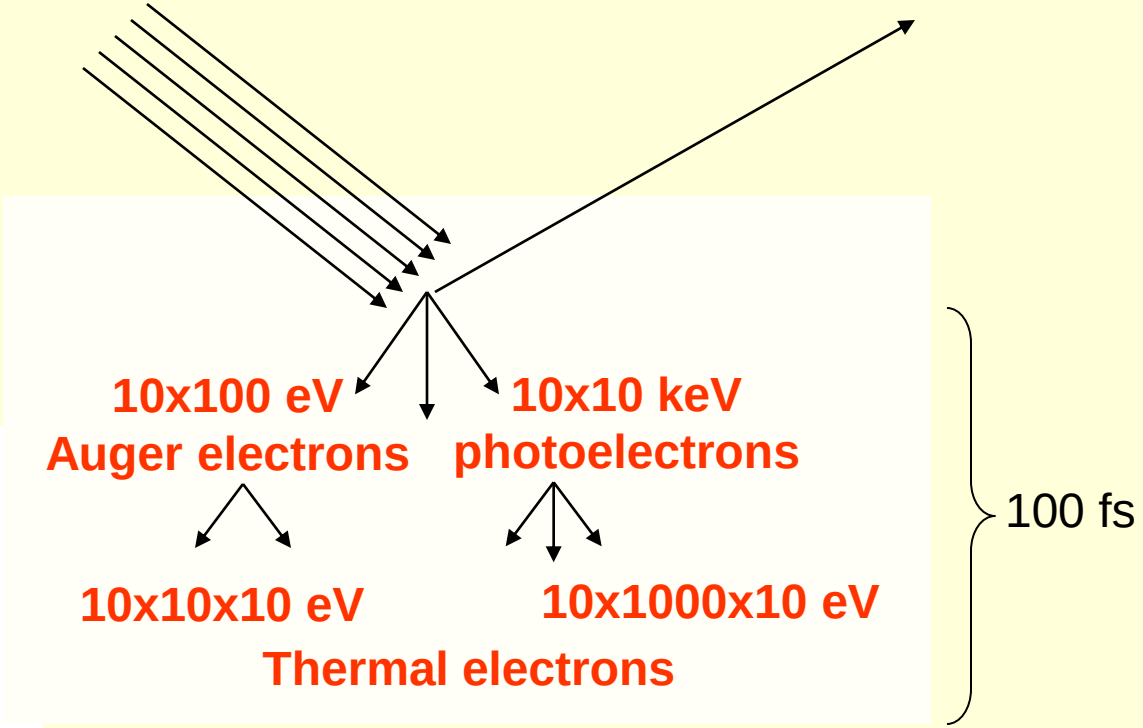

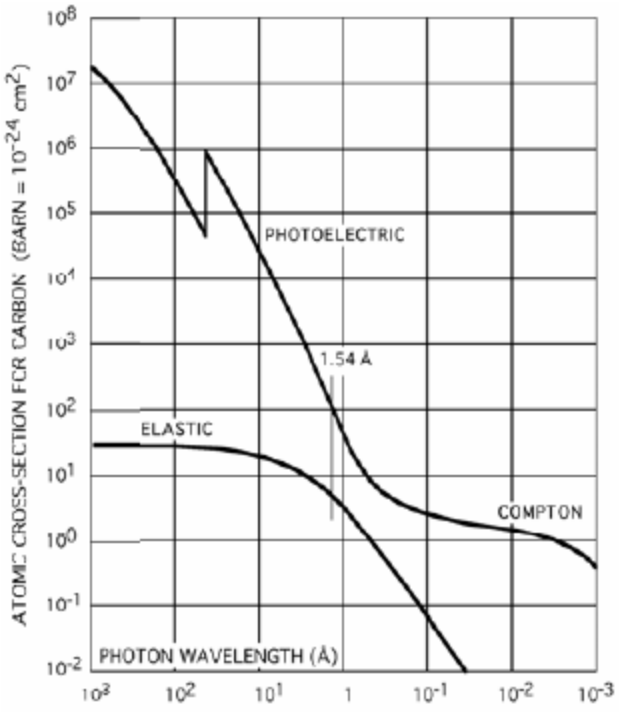

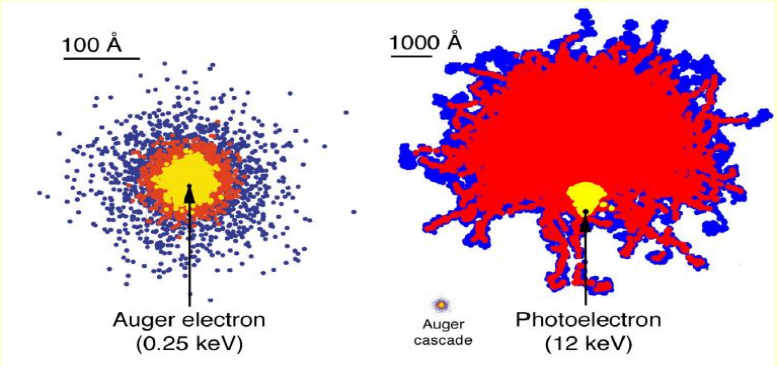

Ziaja et. al, 2000-2002

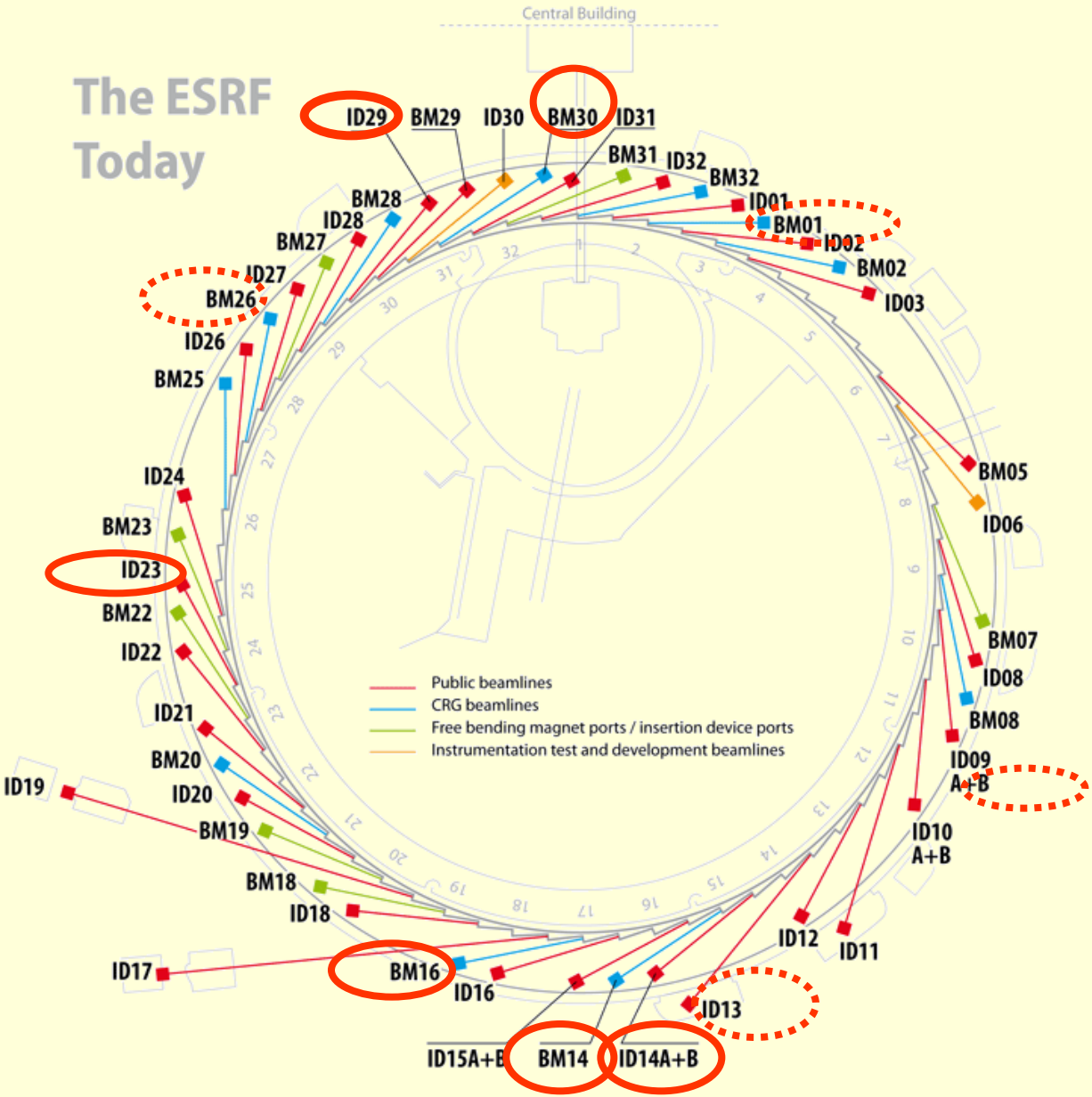
The ESRF
Today
Central Building
ID29
BM29
ID30
BM30
ID31
BM31
ID32
BM32
ID01
BM01
ID02
BM02
ID03
BM05
ID06
BM07
ID08
BM08
ID09
A+B
ID10
A+B
ID11
ID12
ID13
ID14A+B
BM14
ID15A+B
BM16
ID16
ID17
ID18
BM18
BM19
ID19
ID20
BM20
ID21
ID22
BM22
ID23
BM23
ID24
BM25
ID26
BM26
ID27
BM27
ID28
BM28
Public beamlines
CRG beamlines
Free bending magnet ports / insertion device ports
Instrumentation test and development beamlines

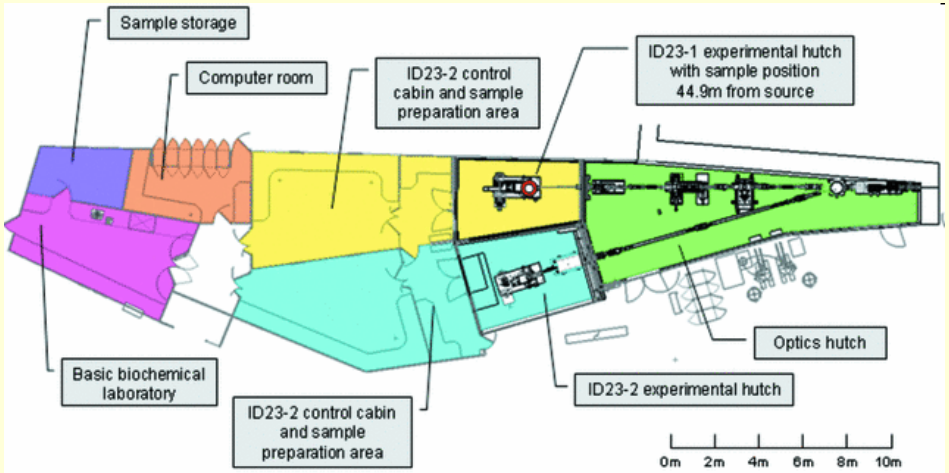
Sample storage
Computer room
ID23-2 control cabin and sample preparation area
ID23-1 experimental hutch with sample position 44.9m from source
Optics hutch
Basic biochemical laboratory
ID23-2 experimental hutch
ID23-2 control cabin and sample preparation area
0m 2m 4m 6m 8m 10m

(*a*)

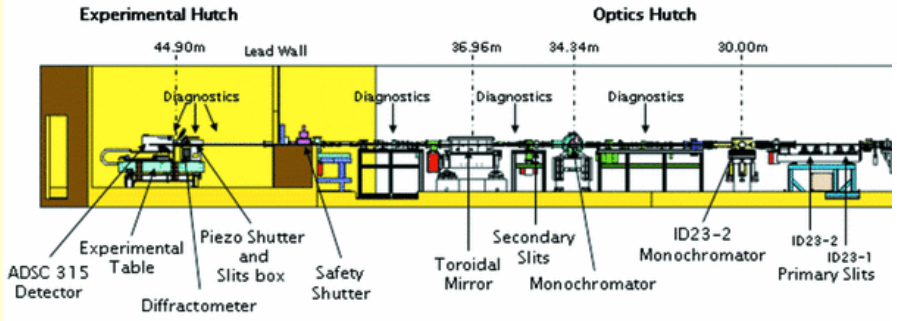
Experimental Hutch
Optics Hutch
44.90m
Lead Wall
36.96m
34.34m
30.00m
Diagnostics
Diagnostics
Diagnostics
Diagnostics
ADSC 315 Detector
Experimental Table
Diffractometer
Piezo Shutter and Slits box
Safety Shutter
Toroidal Mirror
Secondary Slits
Monochromator
ID23-2 Monochromator
ID23-2
ID23-1
Primary Slits

(*b*)

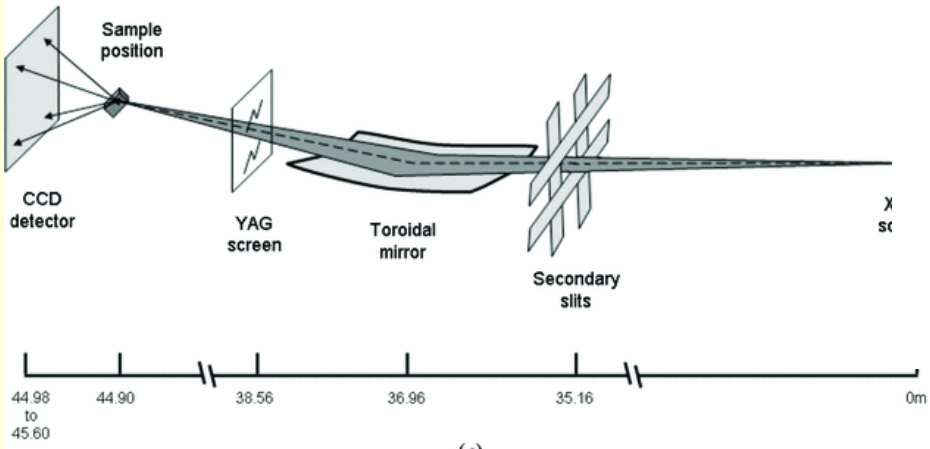
Sample position
CCD detector
YAG screen
Toroidal mirror
Secondary slits
44.98 to 45.60
44.90
38.56
36.96
35.16
0m

(*c*)

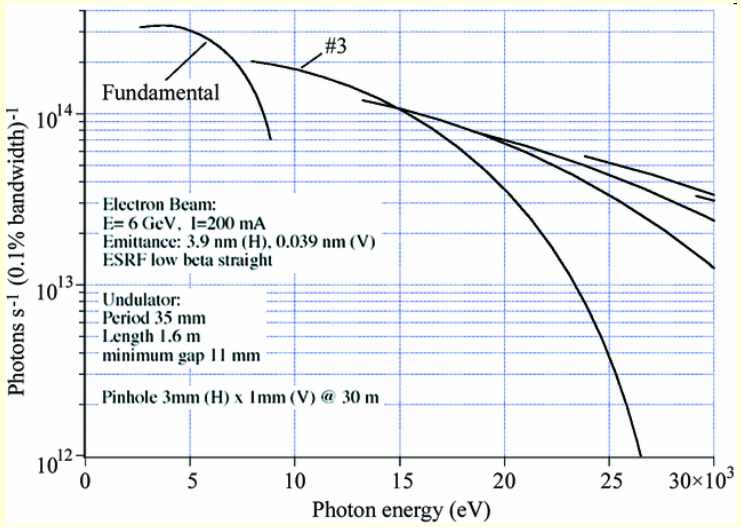
Fundamental
#3
Photons s-1 (0.1% bandwidth)-1
10^14
10^13
10^12
Electron Beam:
E= 6 GeV, I=200 mA
Emittance: 3.9 nm (H), 0.039 nm (V)
ESRF low beta straight
Undulator:
Period 35 mm
Length 1.6 m
minimum gap 11 mm
Pinhole 3mm (H) x 1mm (V) @ 30 m
0 5 10 15 20 25 30×10^3
Photon energy (eV)

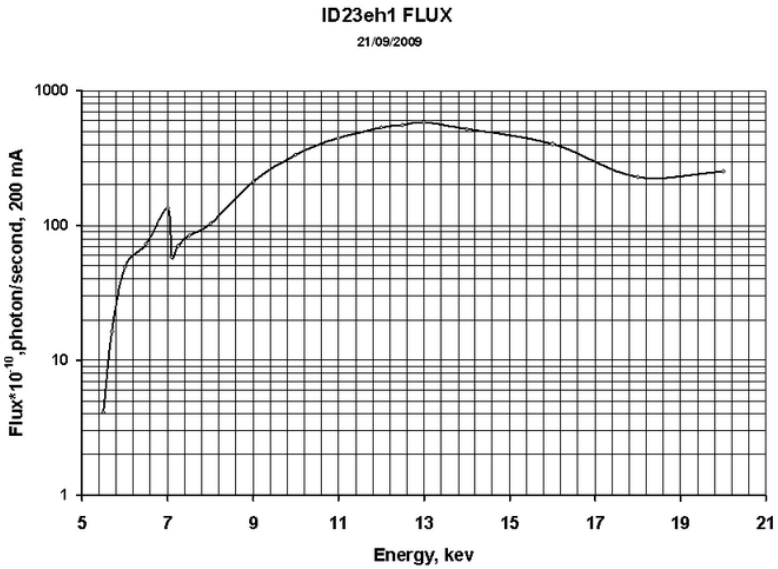
ID23eh1 FLUX
21/09/2009
Flux*10^10,photon/second, 200 mA
1000
100
10
1
5 7 9 11 13 15 17 19 21
Energy, kev

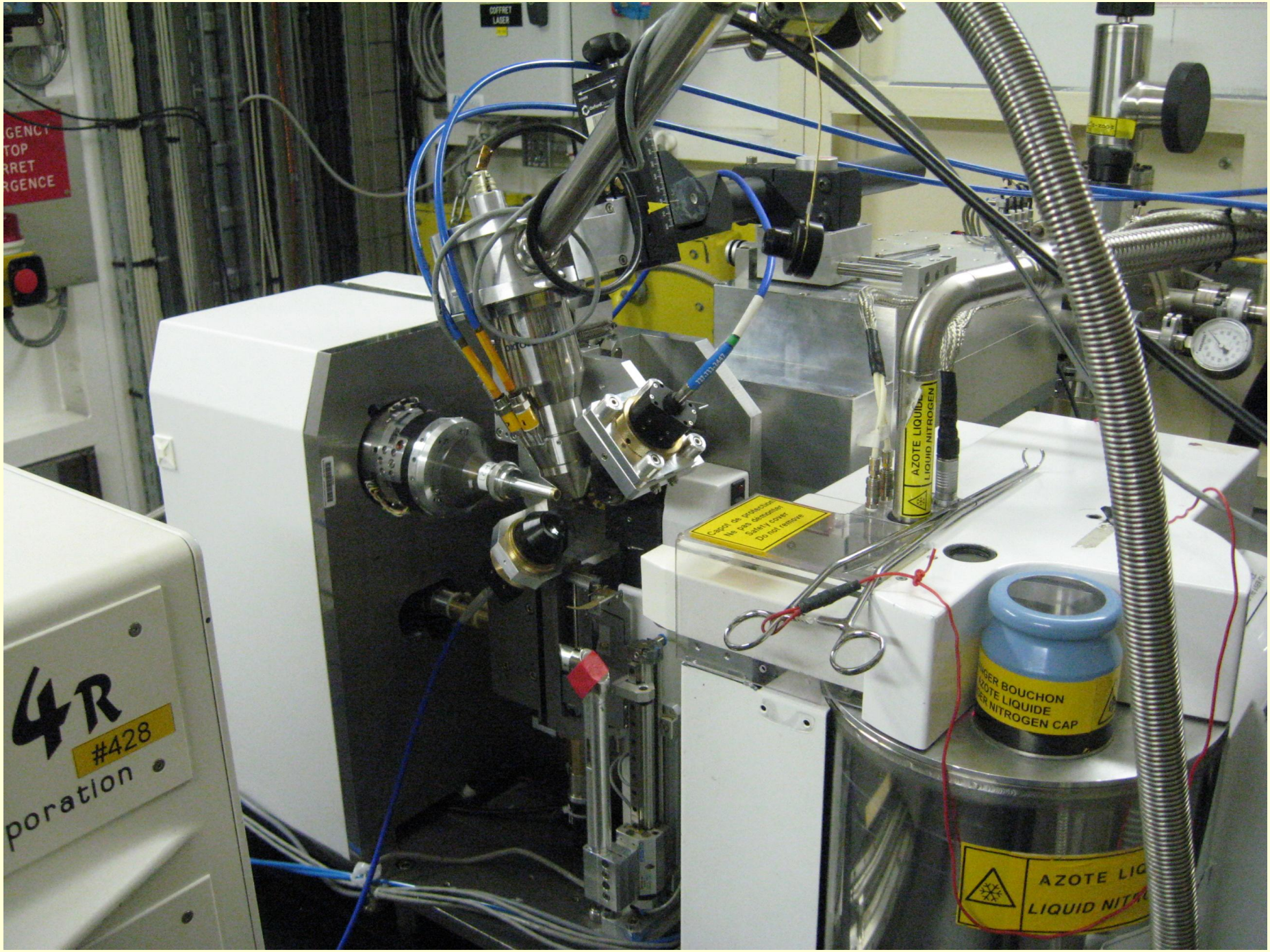
4R
#428
poration
AZOTE LIQUIDE
LIQUID NITROGEN
Caps de protection
Ne pas desserrer
Safety cover
Do not remove
BOUCHON
AZOTE LIQUIDE
NITROGEN CAP
AZOTE LIQ
LIQUID NITR

Ancillary techniques – HC1

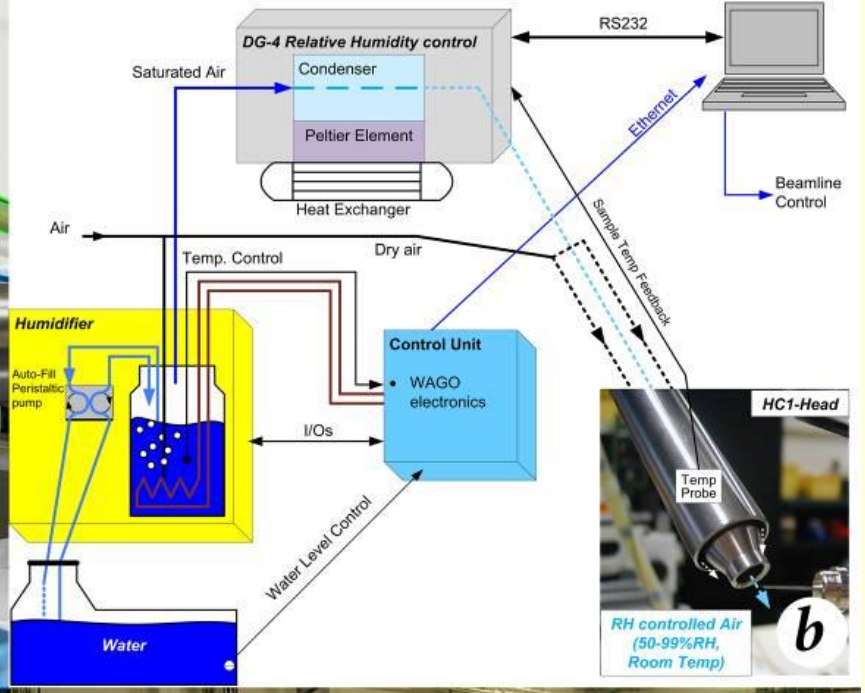

Sanchez-Weatherby *et al.* 2010 *Acta Cryst*. **D65**, 1237-1246

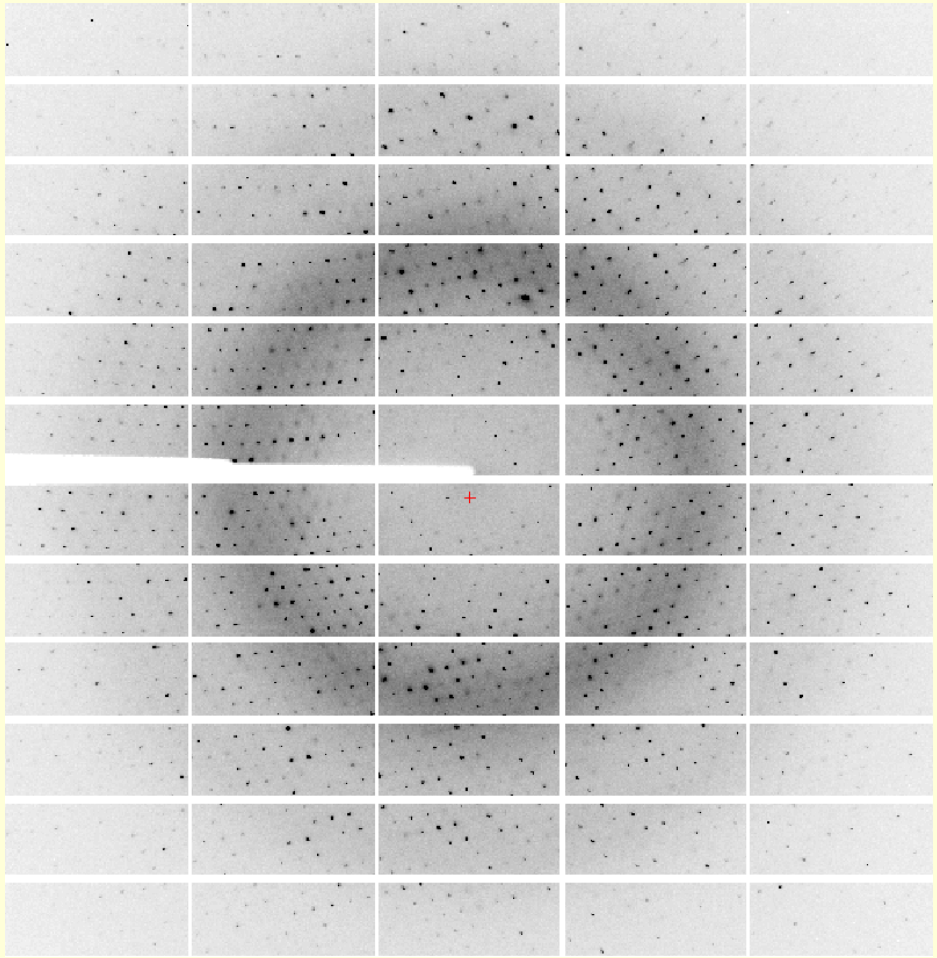

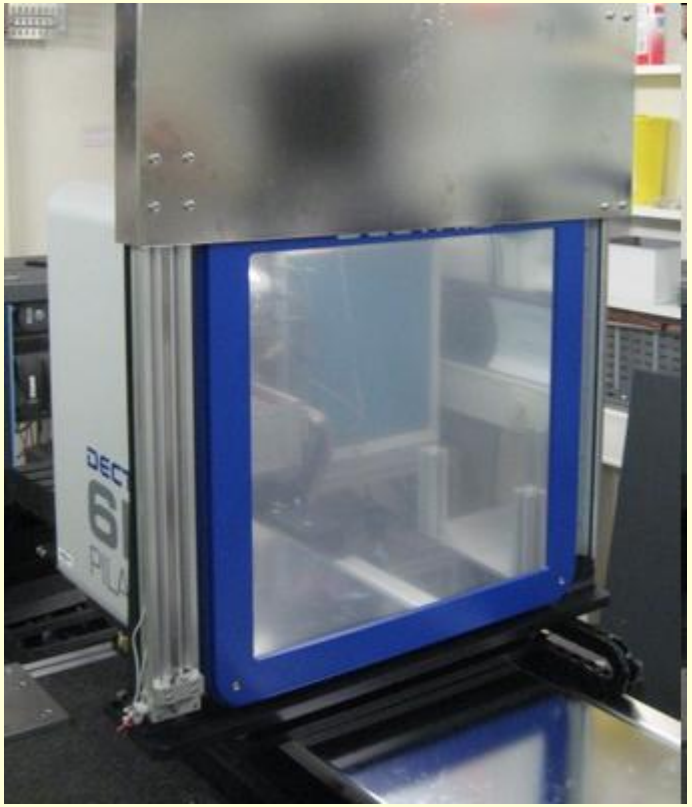

mxCuBE (mx-415)

File Instrumentation Help — Expert mode

Hutch | Collect | Energy scan | XRF spectrum | Image | dna

Phi: -89.4 | 90 — Holder length: 22.73 | 0.1

Available motors: Phi Vertical | Open | -2.935 | 1.0

Minikappa

Motors: omega -89.427 | 90

omega: -89.427 kappa: 0.000 phi: 0.000
-X: -2.220 Y: -1.701 Z: 22.739

Commands: Initialize | Load | Home

Energy — Current: 13.200 keV 0.939 Å — Move to: keV

Transmission — Current: 17.67% — Set to: Filters

Beamstop: in — Safety shutter: closed — Fast shutter: closed

Scan plot

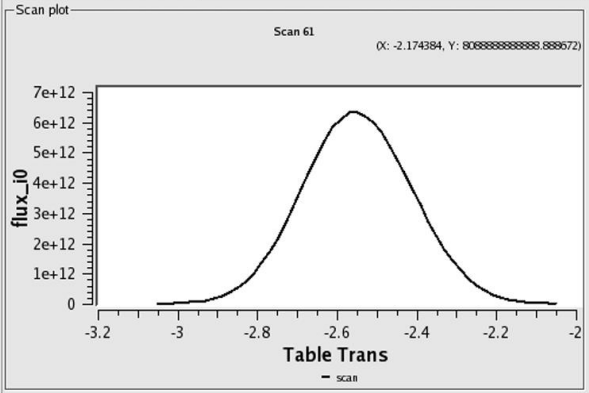

Sample centring: Manual 3-click | Computer automatic | User confirms — Centre | Accept | Reject | Autofocus | Snapshot

Beam commands: Centre beam | Quick realign | Take powders | Anneal

Sample display — Light: 0.45 | 0.1 — Front light: 0.0 | 1.0 — Zoom: 3 — Focus: 0.0 | 0.01

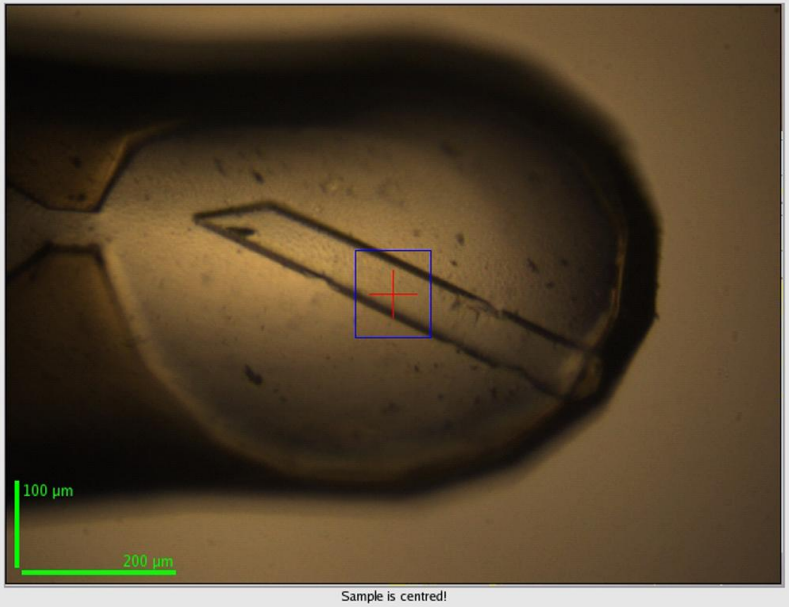

Sample is centred!

Beam size — Hor: 0.1 | 0.01 — Ver: 0.1 | 0.01 — Move | Offsets

ESRF

Machine current: 189.2 mA — 7/8 multibunch — 09:26

Cryo: 100.1 K — 0%
Dry: unknown
Superdry: unknown
Icing: unknown

FAE-X21
1. Preparing beamline
2. Mounting sample
3. Centring sample
4. Collecting images

i0 flux: 0 ph/s

Information messages | Submit feedback | Chat (1) | spec (2377) | DNA log

```
2009-10-26 11:31:19 Image 3: /data/visitor/mx415/id14eh4/20091026/fae/x21/fae-x21_3_003.img (intensity=34963223244387.15625)
2009-10-26 11:31:20 Frame 4, 270.000 to 270.500 degrees
2009-10-26 11:31:22 Integrated counts for image : 3.497e+13
2009-10-26 11:31:22 Image 4: /data/visitor/mx415/id14eh4/20091026/fae/x21/fae-x21_3_004.img (intensity=34970016156621.710938)
2009-10-26 11:31:22 Doing data collection cleanup...
2009-10-26 11:31:24 Collection successful
2009-10-26 11:31:24 No after processAfterCollect information in datacollect xml.
2009-10-26 11:31:24 Data collection successful
2009-10-26 11:33:34 MiniDiff: taking snapshot #1
2009-10-26 11:33:38 MiniDiff: taking snapshot #2
2009-10-26 11:33:40 MiniDiff: taking snapshot #3
2009-10-26 11:33:43 MiniDiff: taking snapshot #4
```

Current users — Selecting gives control — Allow timeout control — Ask for control — My name: artemis2

Oct 26 09:05 Delivery:Next Refill at 21:00;

spec: eh4

Transport and ship in LN2

- Dry shipper
- Foam insulation
- Pour off LN2
- Fedex, Airborne
- Checked luggage
- Get the paperwork

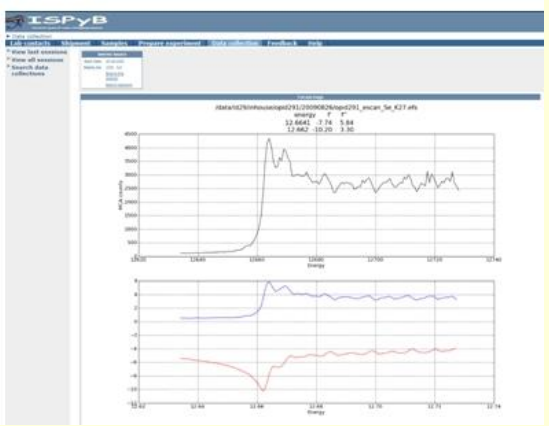
ISPyB


Crystal Snapshots

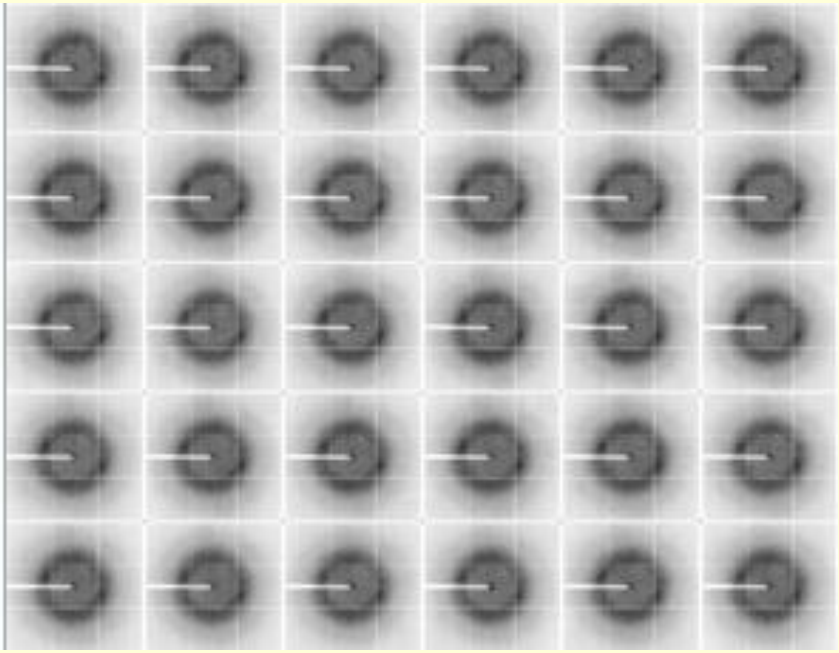

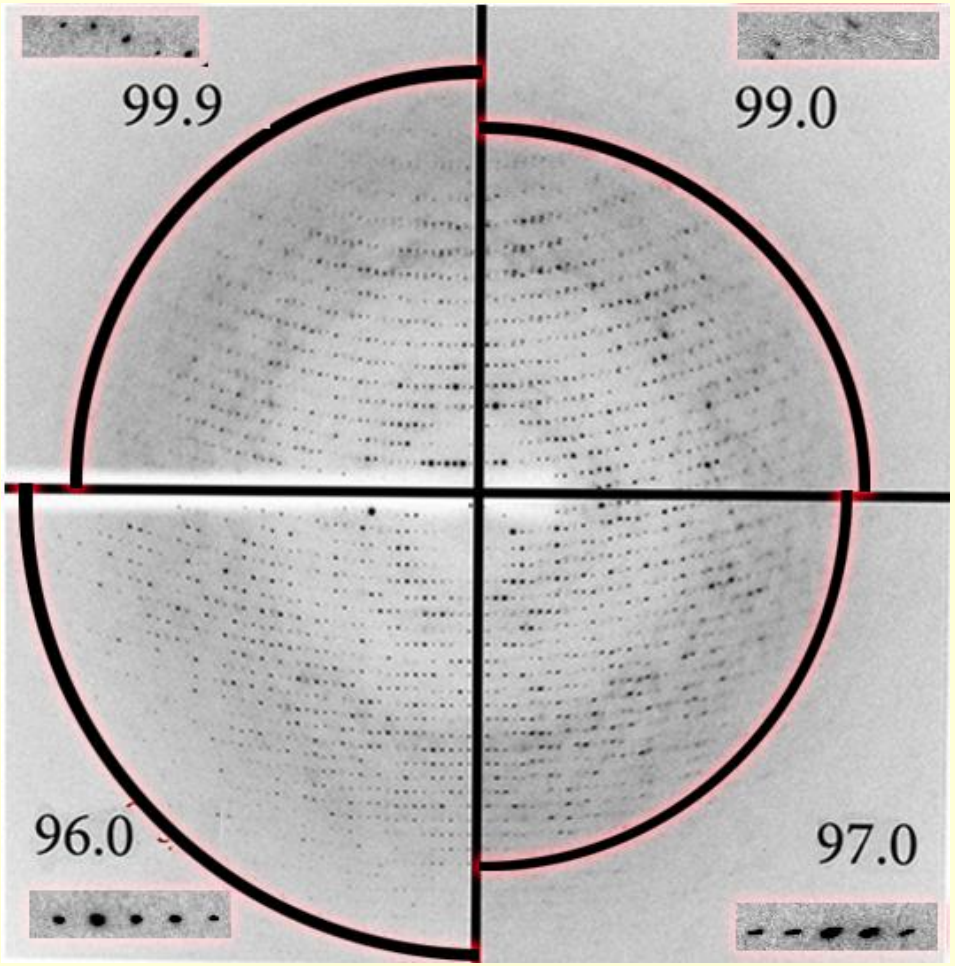

Sanchez-Weatherby *et al.* 2010 *Acta Cryst*. **D65**, 1237-1246

ESRF Upgrade

MASSIV

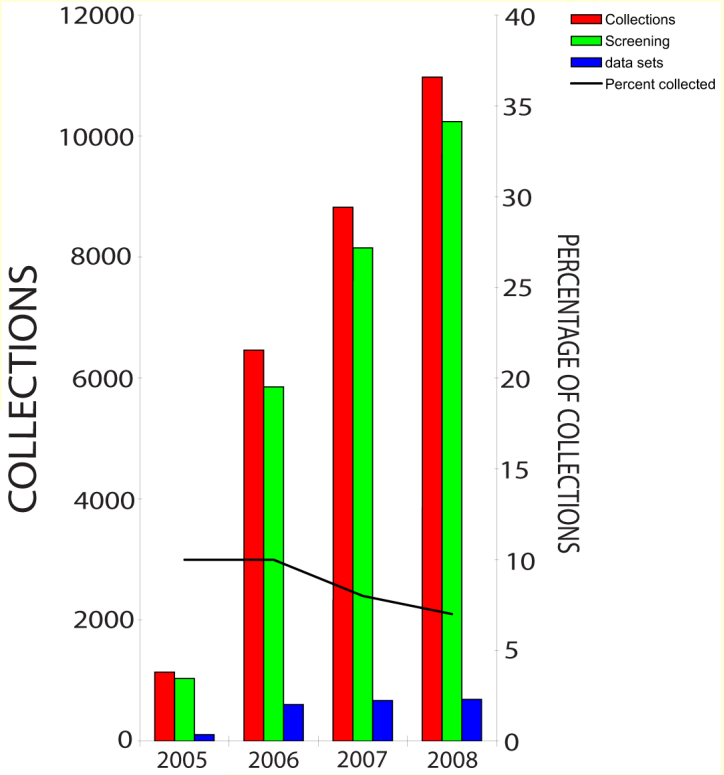

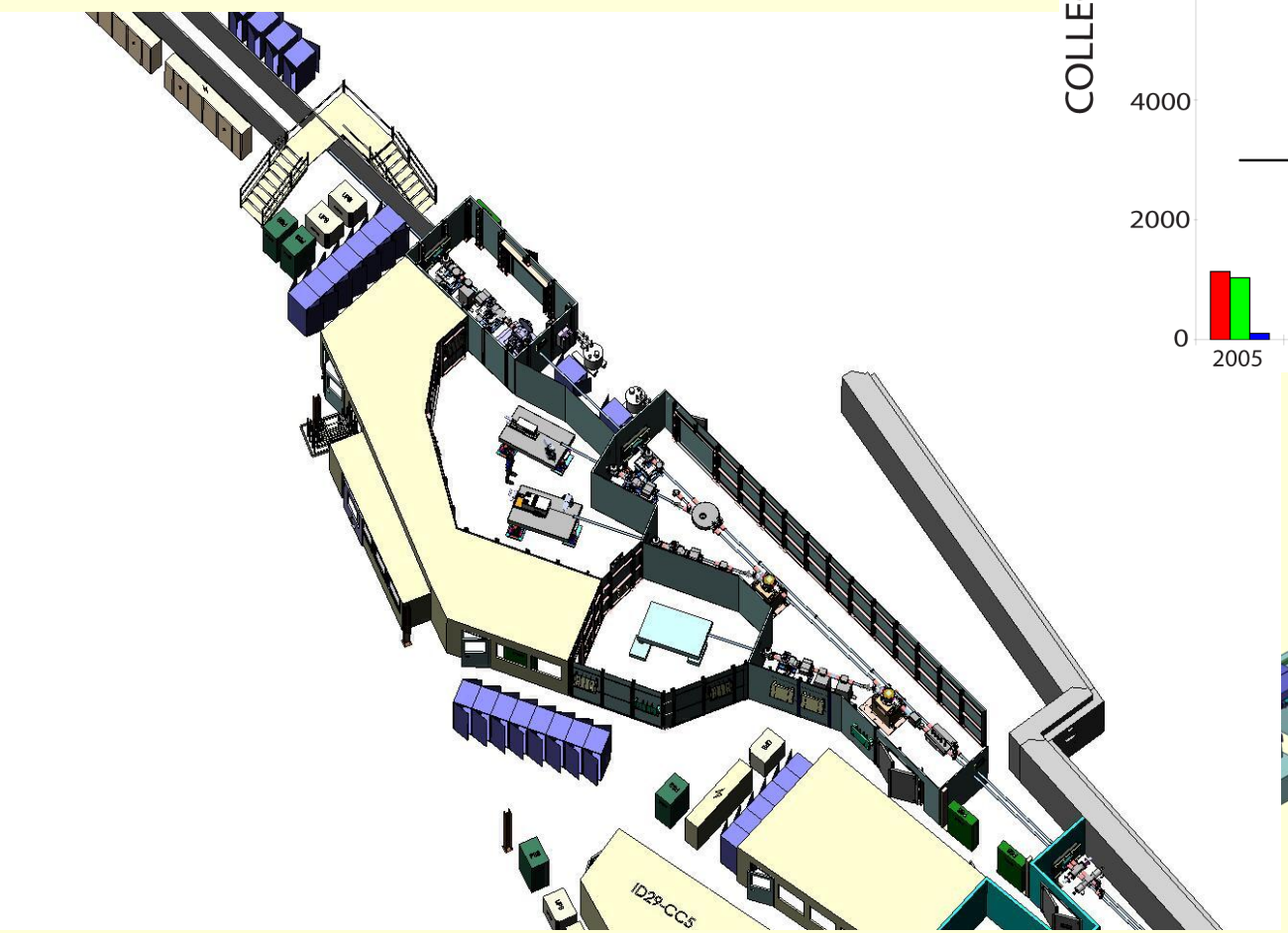

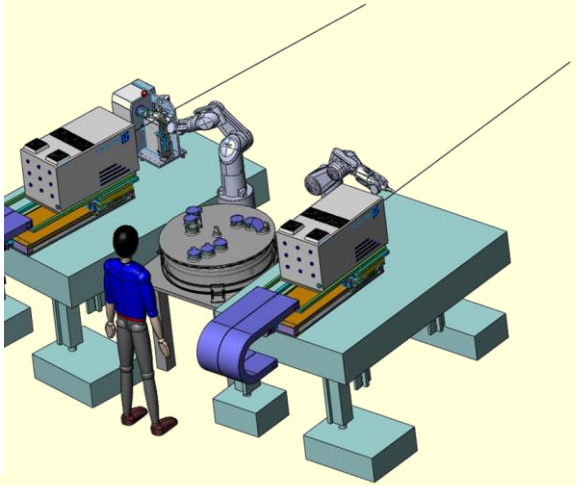

proteins are dynamic molecules

- enzymes, sensor proteins, inhibitors, etc.
- standard crystallography only gives static picture
- how does the structure of the molecule change along its reaction pathway?

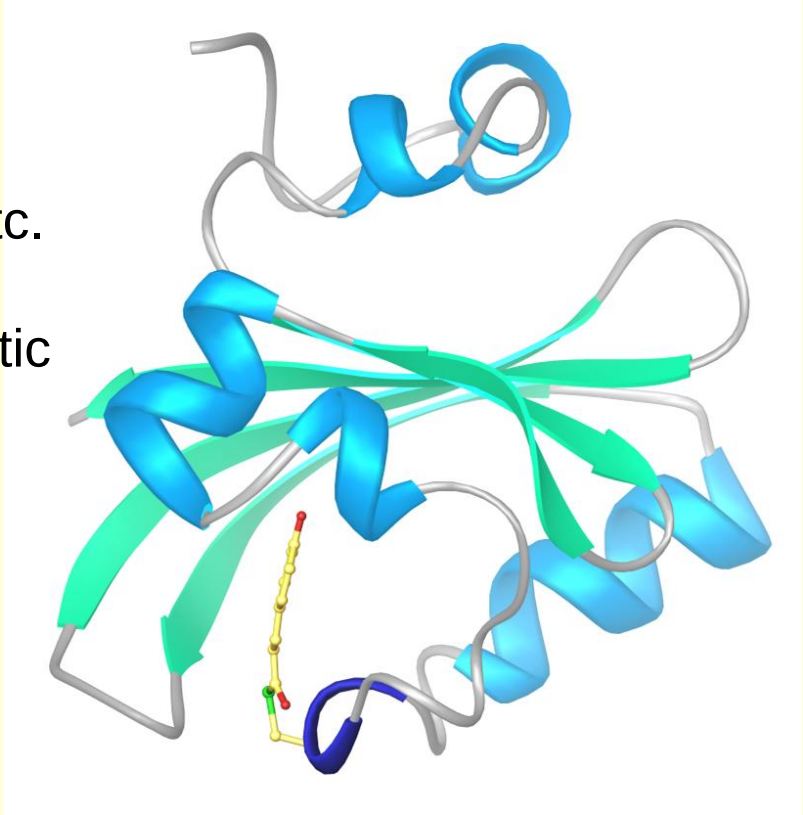

Structure of the blue light sensor, photoactive yellow protein (PYP)

Borgstahl et al., Biochemistry (1995) **34,** 6278–6287

Laue crystallography

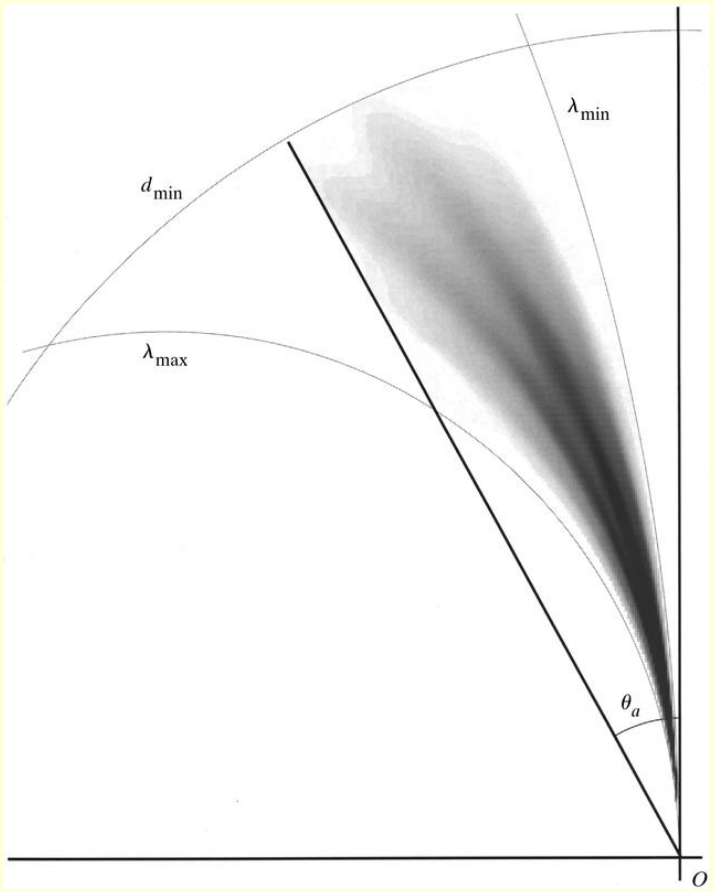

Probability distribution of measurable reflections in reciprocal space.

Ren et al., J. Synchrotron Rad. (1999) **6,** 891–917.

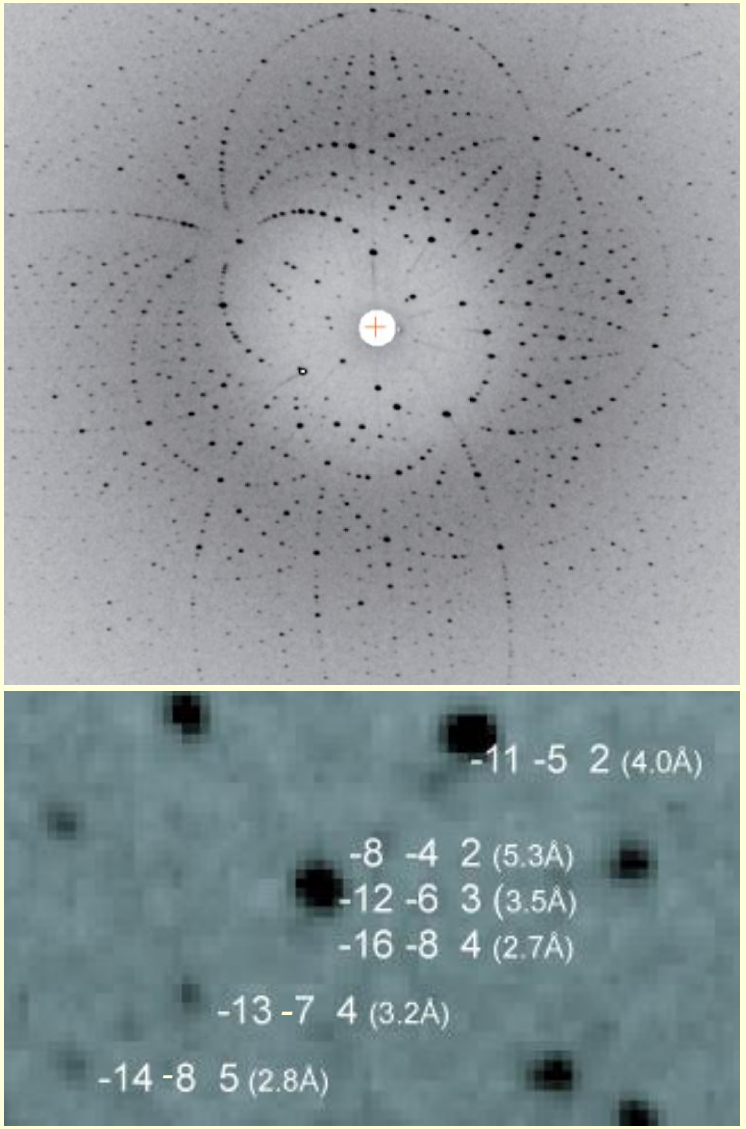

HKL assignments and resolution of reflections in an ellipse. Multiple assignments for a single spot indicates harmonically overlapped reflections.

X-ray probe

- length of X-ray exposure is dependent on time resolution

- short monochromatic oscillation exposures are adequate for long biological reactions

- most systems demand the use of Laue crystallography

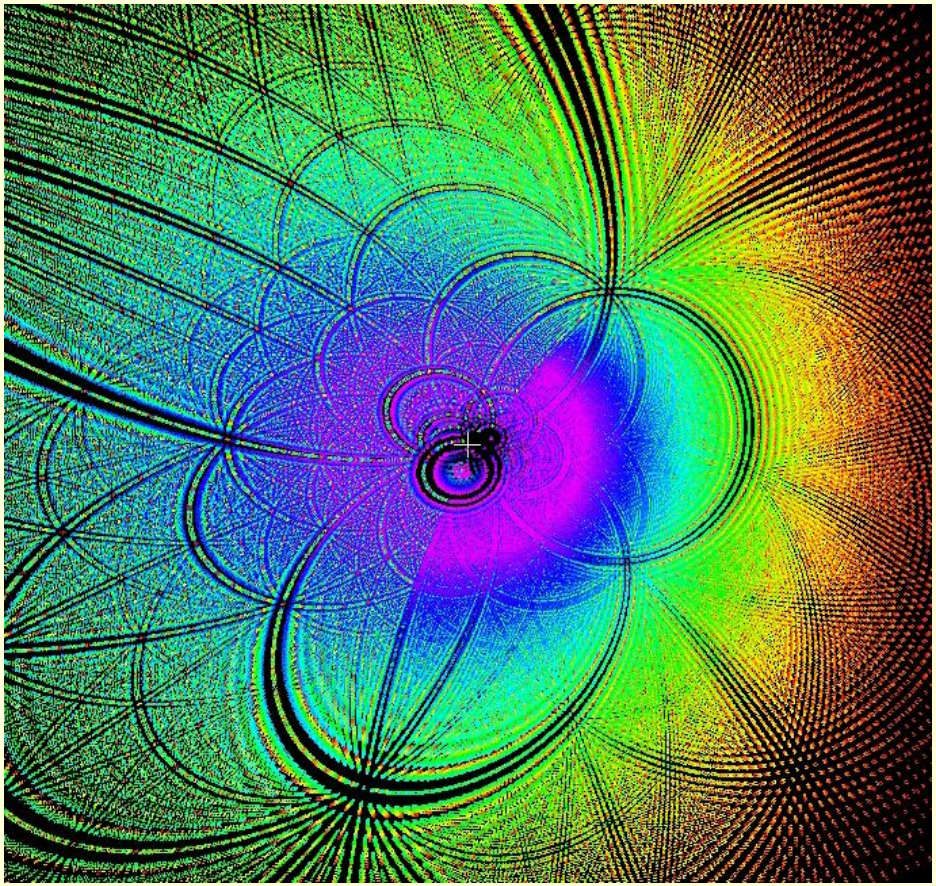

theoretical Laue diffraction pattern with the reflection color coded according to the wavelength

synchrotron bunch structure

- necessary bunch length dependent on desired time resolution
- maximize current to minimize exposures
- ~100mA total current in all modes

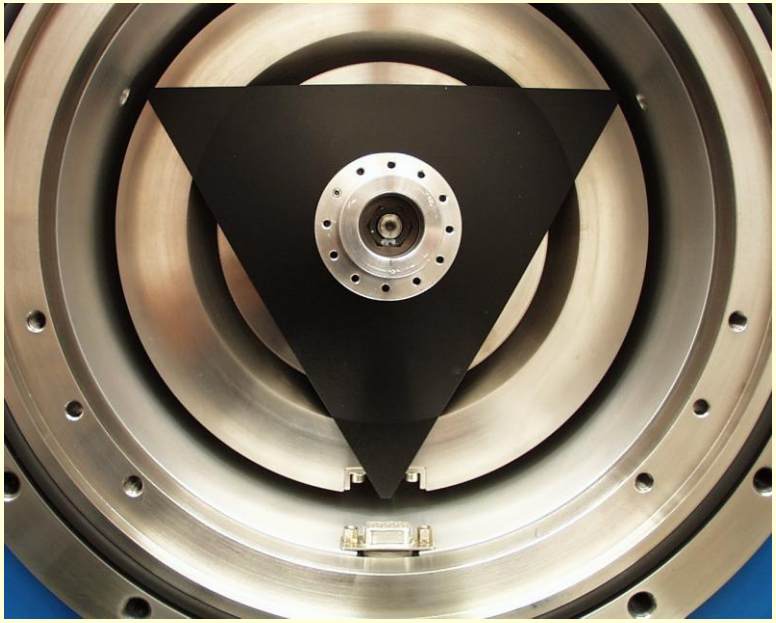

Jülich fast shutter, ~ 2µs minimum open-time at 900Hz

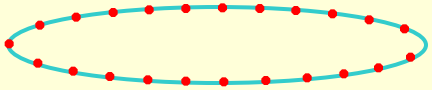

24 bunches

Standard operating mode- singlets only

- 3.68µs for single revolution
- ~4mA per bunch

~8mA

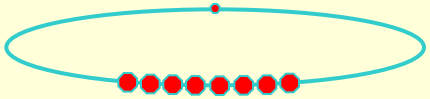

8 x 7 bunches

Special operating mode- hybrid/singlet

- ~100ps: X-ray pulse duration
- ~500ns: X-ray pulse duration of the 8x7 “super-pulse”

experimental setup

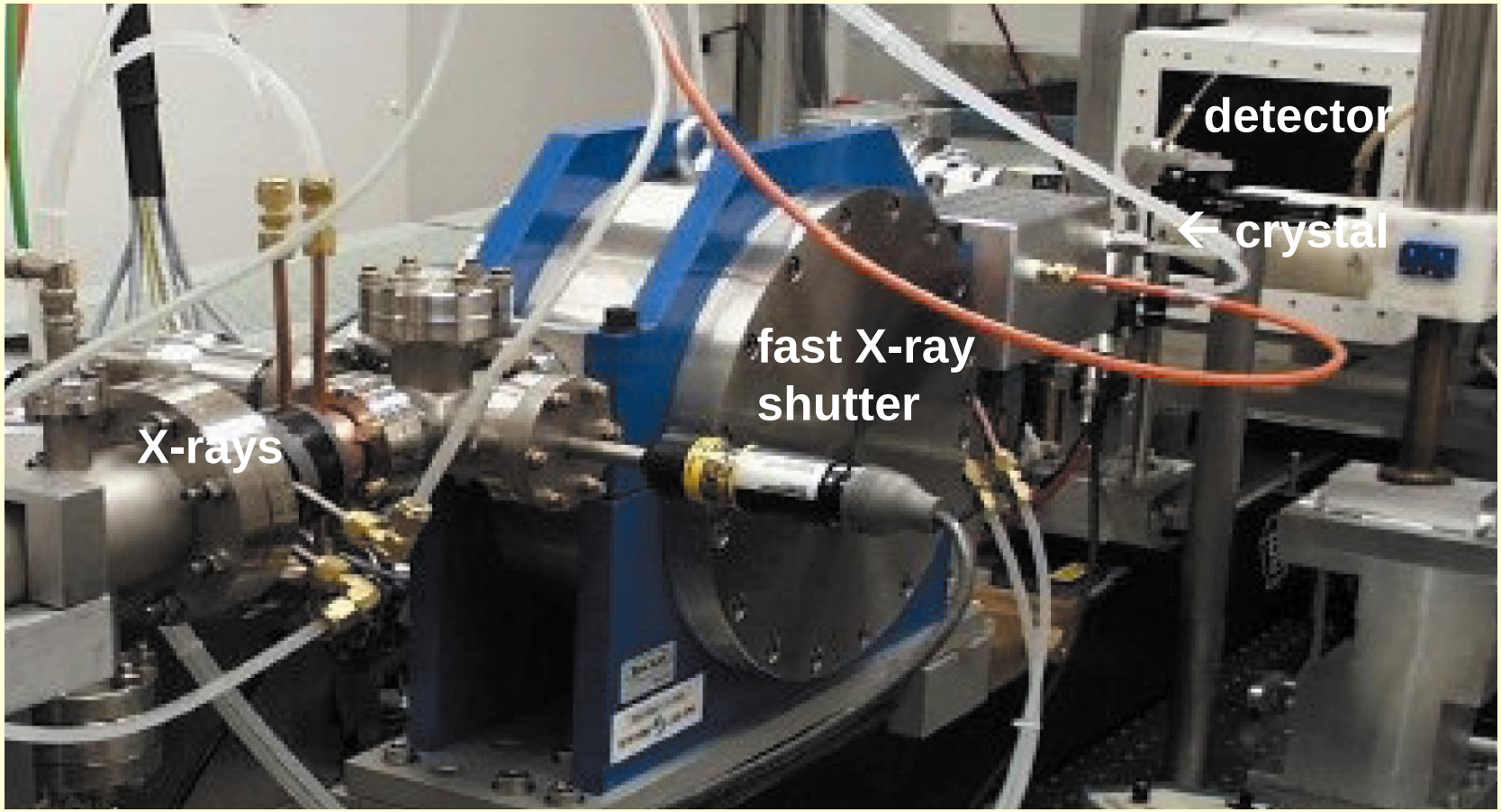

Pump-probe experiments and time-resolved diffraction

Pico-second Crystallography

Myoglobin in Action

Snapshot of myoglobin MbCO taken 100 picoseconds after the dissociation of CO was triggered by a flash of light from a femtosecond laser. Blue and red colours show regions where the protein gained or lost electron density.

By recording Laue images as a function of the delay from the laser flash, the change in the electron density is mapped as a function of time

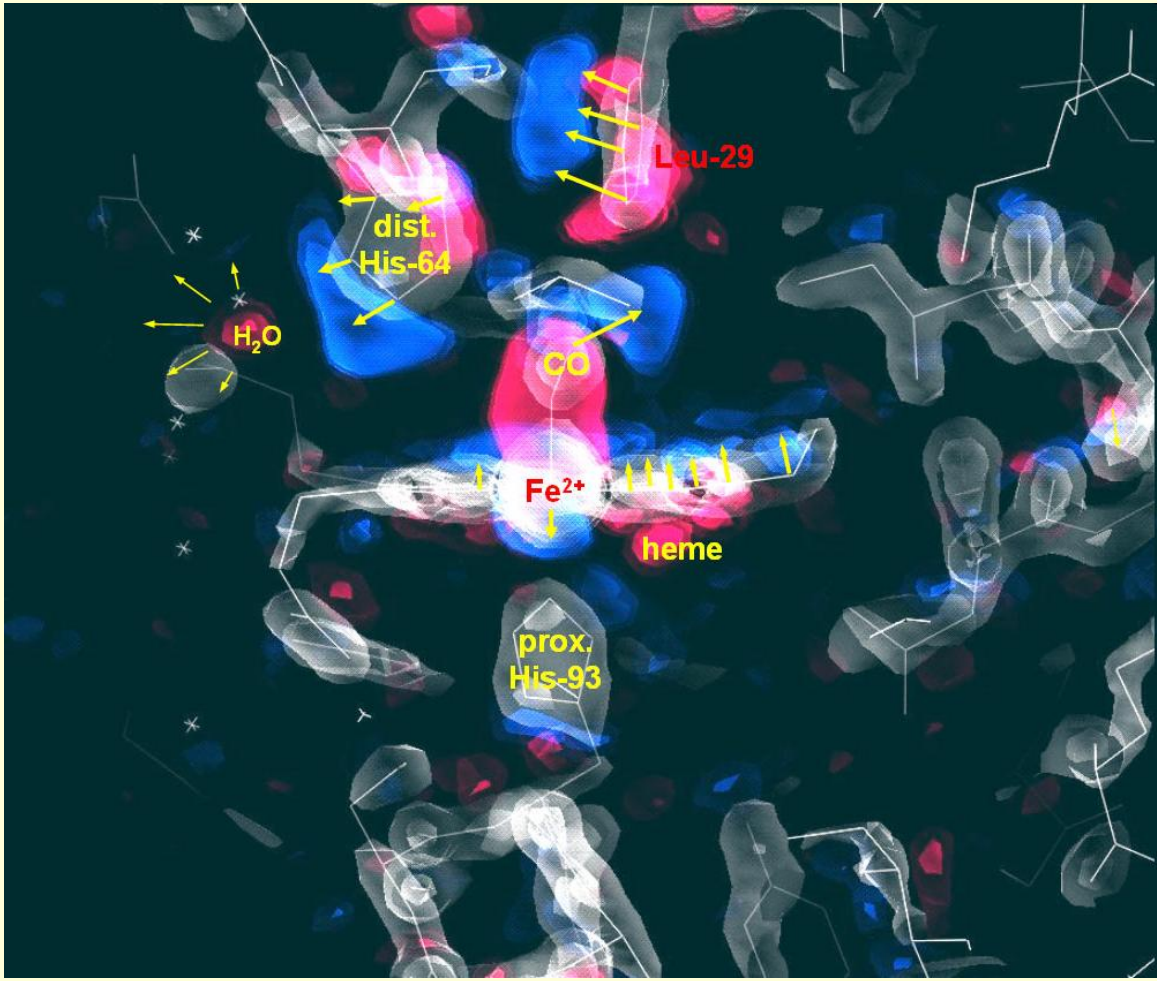

F. Schotte et al. *Science*, 300, 1944-1947 (2003)

Snapshots of a photosynthetic reaction centre

Time-resolved Laue diffraction snapshots can show movement of atoms and changes

in electron density on a millisecond time scale

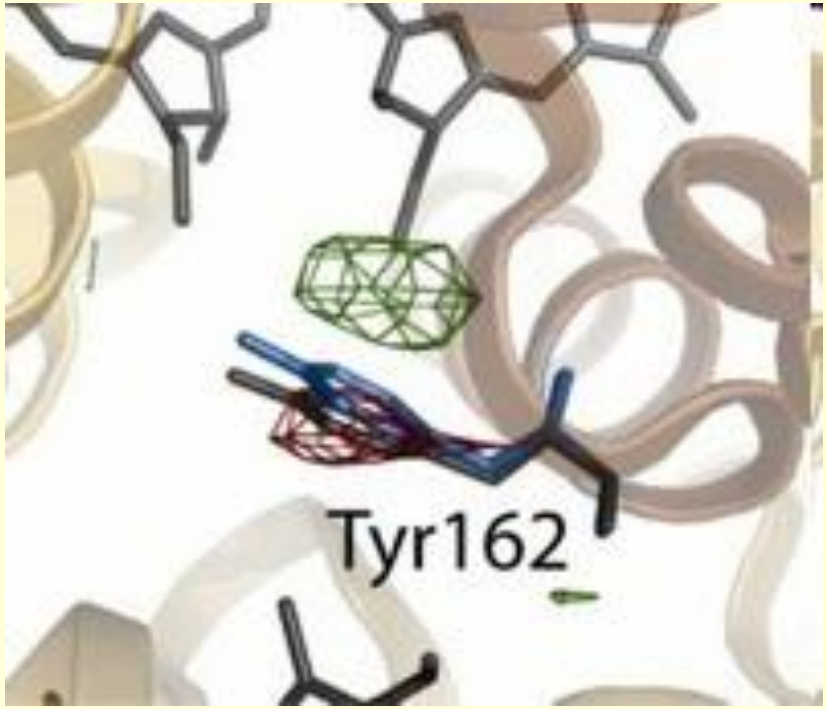

Overview of the structure and energy transfer reactions of the bacterial photosynthetic reaction centre of Blastochloris viridis. Light causes electrons to move from the special pair (P960) to quinone molecules (QA and QB) on the opposite side of the membrane. P+960 is, in turn, reduced from the tetra-heme cytochrome subunit.

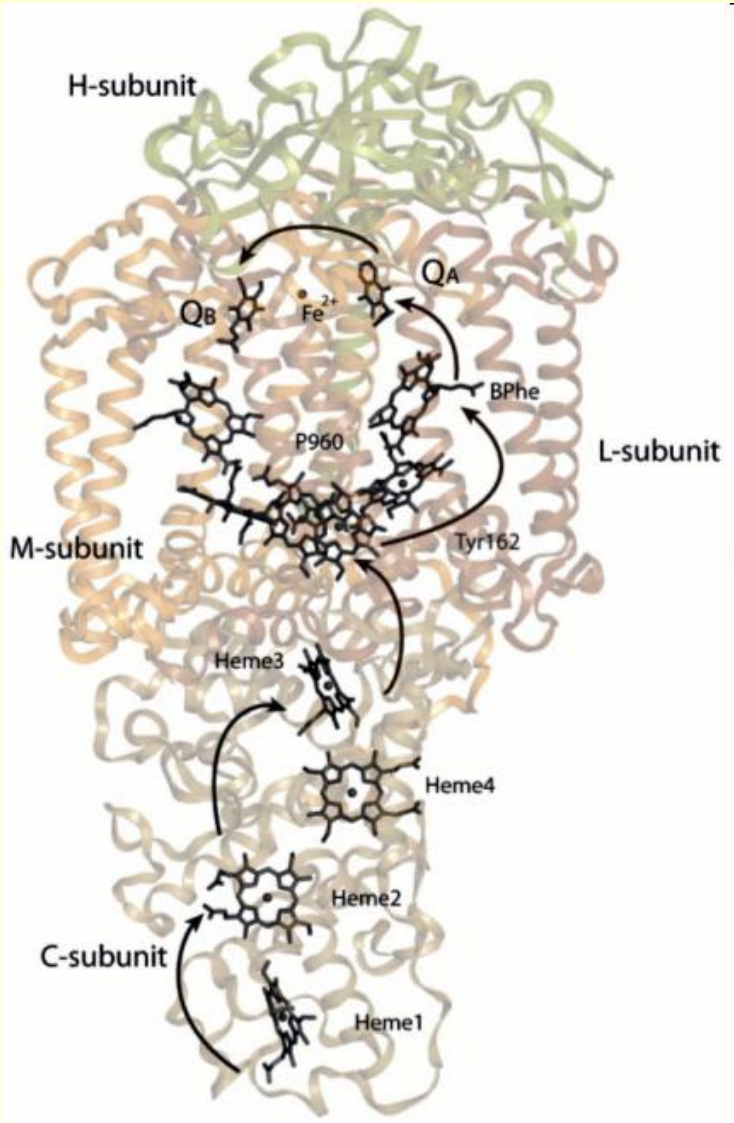

A.B. Wöhri et all.
Light-induced structural changes in a photosynthetic reaction center caught by Laue diffraction,
***Science* 328, 630-633 (2010).**

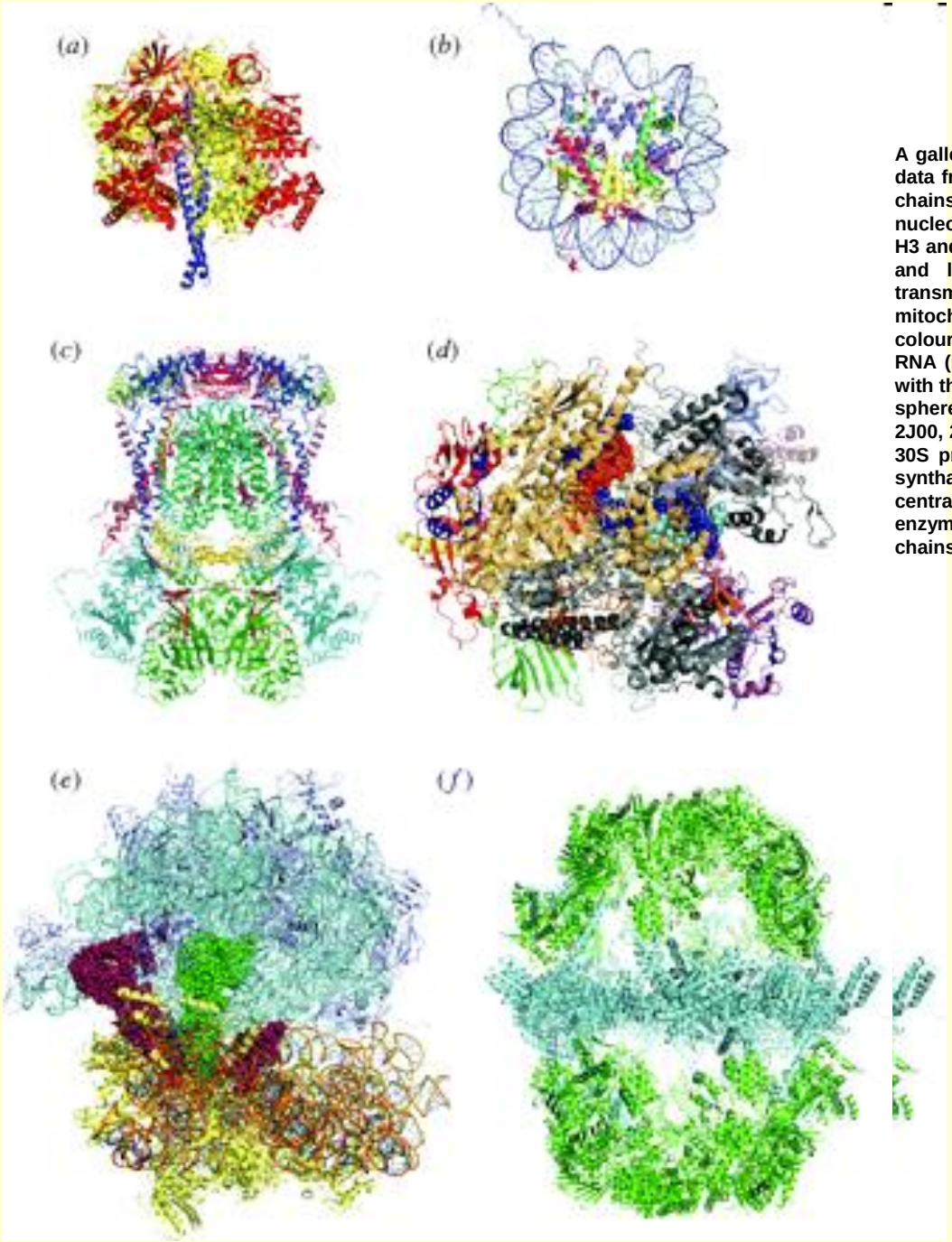

A gallery of selected important large biological structures that have been solved with data from SR sources. (*a*) F1-ATPase (351 kDa; PDB ID 1BMF). The three non-active α chainsare in red, the three active β chains in yellow and the γ subunit in blue. (*b*) The nucleosome core particle (206 kDa; PDB ID 1AOI). The four histone proteins, H2A, H2B, H3 and H4, are in pink, yellow, blue and green, respectively and 146 bp of DNA in dark and light blue. (*c*) Cytochrome BC1 complex (480 kDa; PDB ID 1BE3). The transmembrane region is in the centre and the matrix space below. The bovine mitochondrial protein is a dimer and the 11 different subunits are shown in different colours. (*d*) RNA polymerase II in complex with DNA (dark and light blue spheres) and RNA (red spheres) (500 kDa; PDB ID 1Y1W). The 12 subunits are in different colours with the major subunit Rpb1 in grey. (*e*) The 70S ribosome in complex with tRNA (green spheres for the P site and dark red spheres for the A and E sites) (2500 kDa; PDB ID 2J00, 2J01). The 50S proteins and RNA are in light blue and cyan, respectively, and the 30S proteins and RNA in pale yellow and orange, respectively. (*f*) Fungal fatty acid synthase (2600 kDa; PDB ID 2UV9, 2UVA). The six α subunits are in cyan and form a central wheel. The six β subunits are in green. The enzyme contains six different enzyme activities at different sites within the large (210 kDa and 230 kDa) polypeptide chains.

Structure and function of the ribosome

In 2009 Nobel Prize in Chemistry is awarded to **Venkatraman Ramakrishnan**, **Thomas A. Steitz** and **Ada E. Yonath** for their studies of the structure and function of the ribosome.

DNA(gene) →*transcription*→RNA(mRNA)->>>*translation*>>>Protein

The central dogma (Crick, 1970) of molecular biology in its simplest form

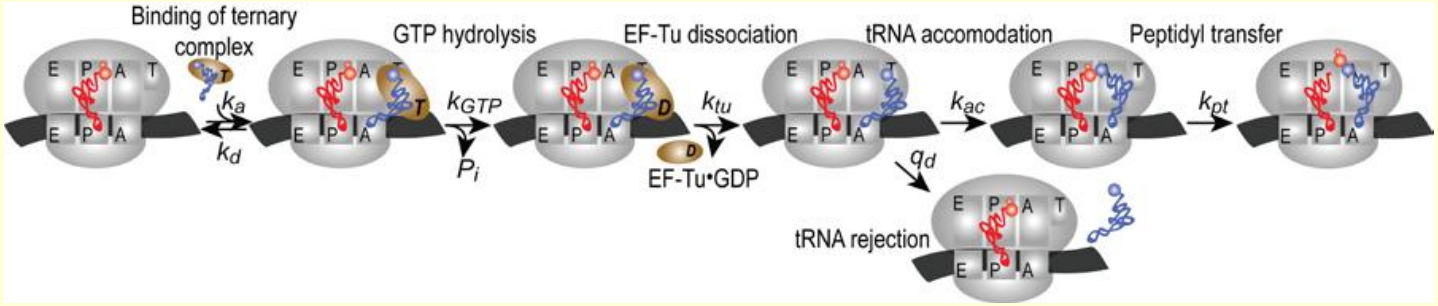

Scheme for ribosomal decoding and peptidyl-transfer. Ternary complex binds to the ribosomal A site with rate constant *ka* and dissociates with rate constant *kd*. GTP on EF-Tu is hydrolyzed with rate constant *kGTP*, EF-Tu leaves with rate constant *ktu*, tRNA accommodates in the A site with rate constant *kac* or dissociates by proofreading with rate constant *qd* and peptidyl-transfer occurs with rate constant *kpt*. The tRNAs are drawn to show their familiar L-shape, rather than their exact orientation on the ribosome.

Components of the ribosome. The bacterial (70S) ribosome consists of a small (30S) and a large (50S) subunit, with molecular weights of about 800 000 and 1 500 000 Dalton (Da), respectively, where S stands for the Svedberg unit for sedimentation velocity. The 30S subunit consists of about 20 different proteins and a sequence, 16S, of ribosomal RNA (rRNA) containing about 1600 nucleotides. The 50S subunit consists of about 33 different proteins, a 23S rRNA sequence with about 2900 nucleotides, and a 5S rRNA sequence with about 120 nucleotides.

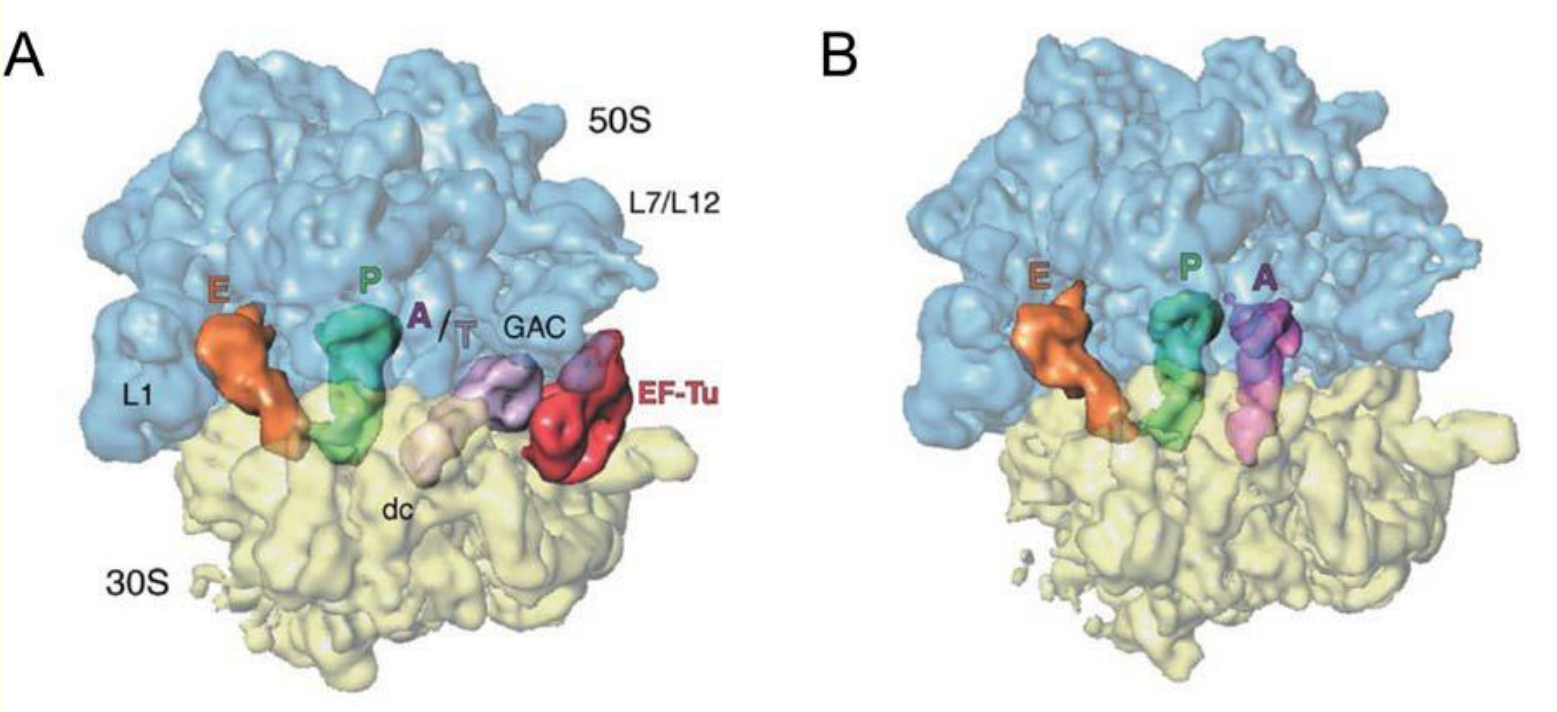

Binding of EF-Tu and tRNAs to the ribosome seen by cryo-EM. (A) Aminoacyl-tRNA in A/T site in ternary complex, peptidyl-tRNA in P site and deacylated tRNA in E site. (B) Pre-translocation ribosome with peptidyl-tRNA in A site, deacylated tRNAs in P and E site (From Valle et al., 2003).

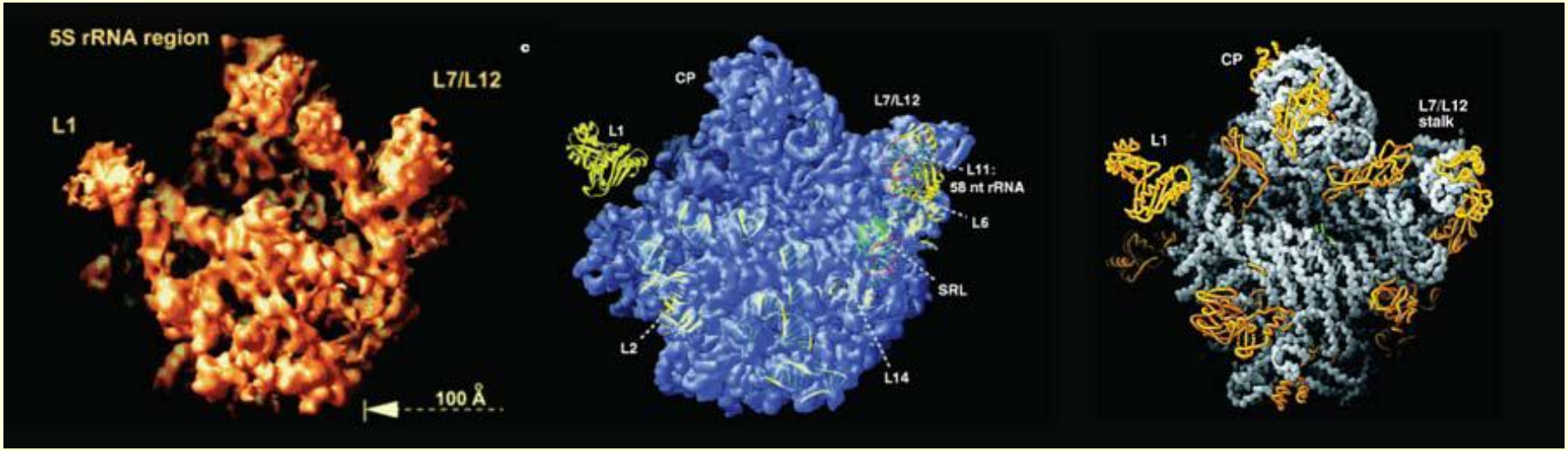

The path to the 50S subunit structure at high resolution. The 50S subunit structure at 9Å resolution (left, 1998), 5Å resolution (middle, 1999) and 2.4Å resolution (right, 2000) (From Ban et al., 1998; 1999; 2000).

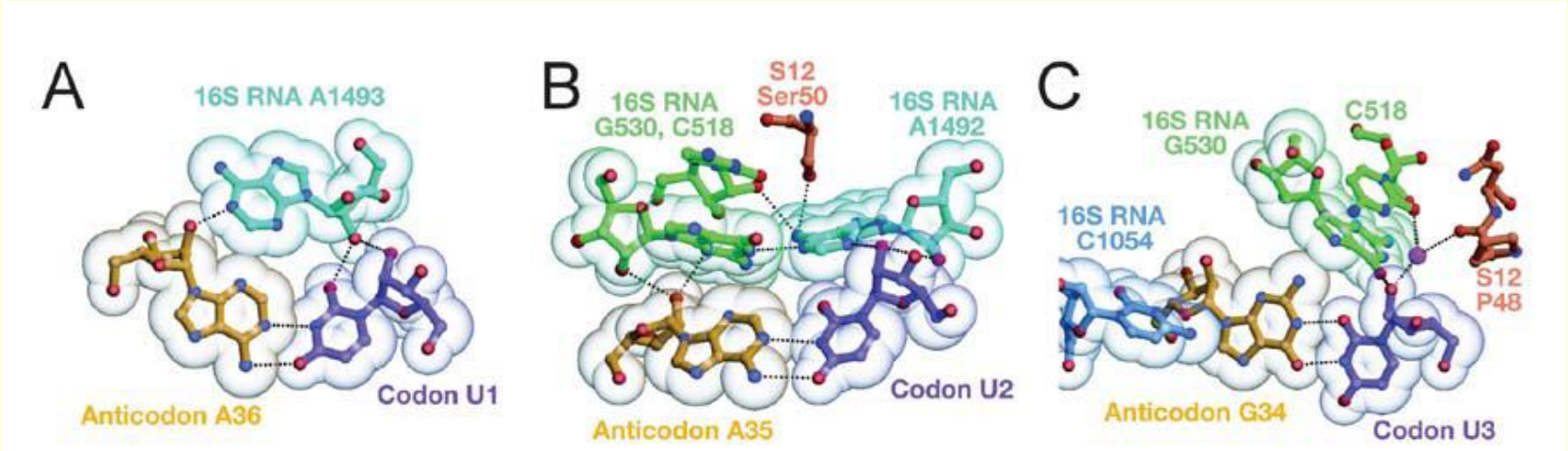

How the ribosome increases the intrinsic selectivity, *d*, of codon recognition. (A) The geometry of base pairing between U1 in first codon position and A36 in the anticodon is monitored by A1493. (B) The geometry of base pairing between U2 in second codon position and A35 in aminoacyl-tRNA is monitored by A1492 and G530, while the geometry of the base pairing in third codon position (U3:G34) is less stringently monitored, explaining the wobble hypothesis (From (Ogle and Ramakrishnan, 2005)).

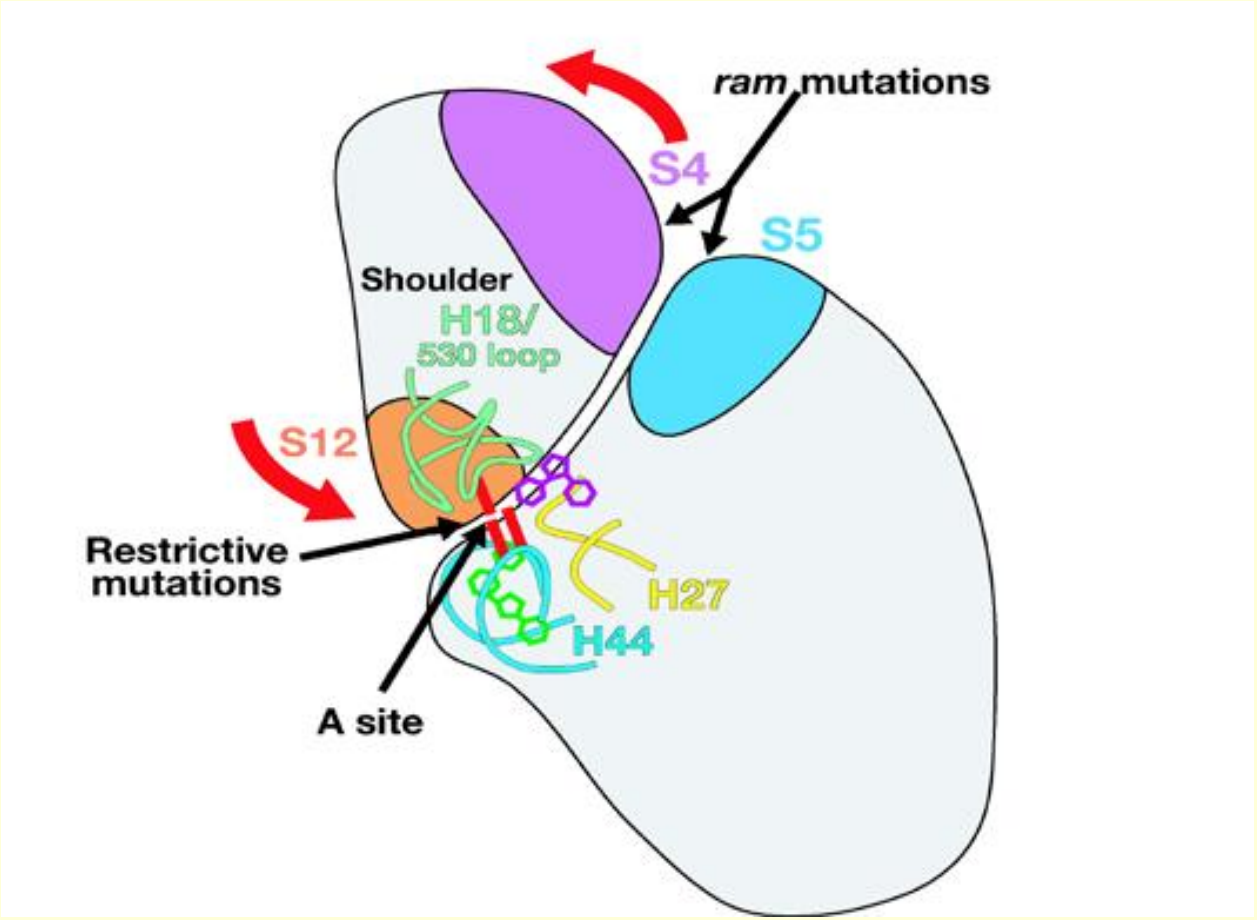

Closing and opening of the 30S subunit. The subunit opens and closes by intra-subunit rotations (red arrows) around the A site The open conformation is stabilized by ribosomal proteins S4 and S5, while the closed conformation is stabilized by ribosomal protein S12. Cognate aminoacyl-tRNAs and some error inducing drugs (e.g. paromomycin) stabilize the closed conformation. Mutations in S12 tend to stabilize the open conformation (increased accuracy) and mutations in S4 and S5 tend to stabilize the closed conformation (decreased accuracy) (From (Ogle and Ramakrishnan, 2005)).

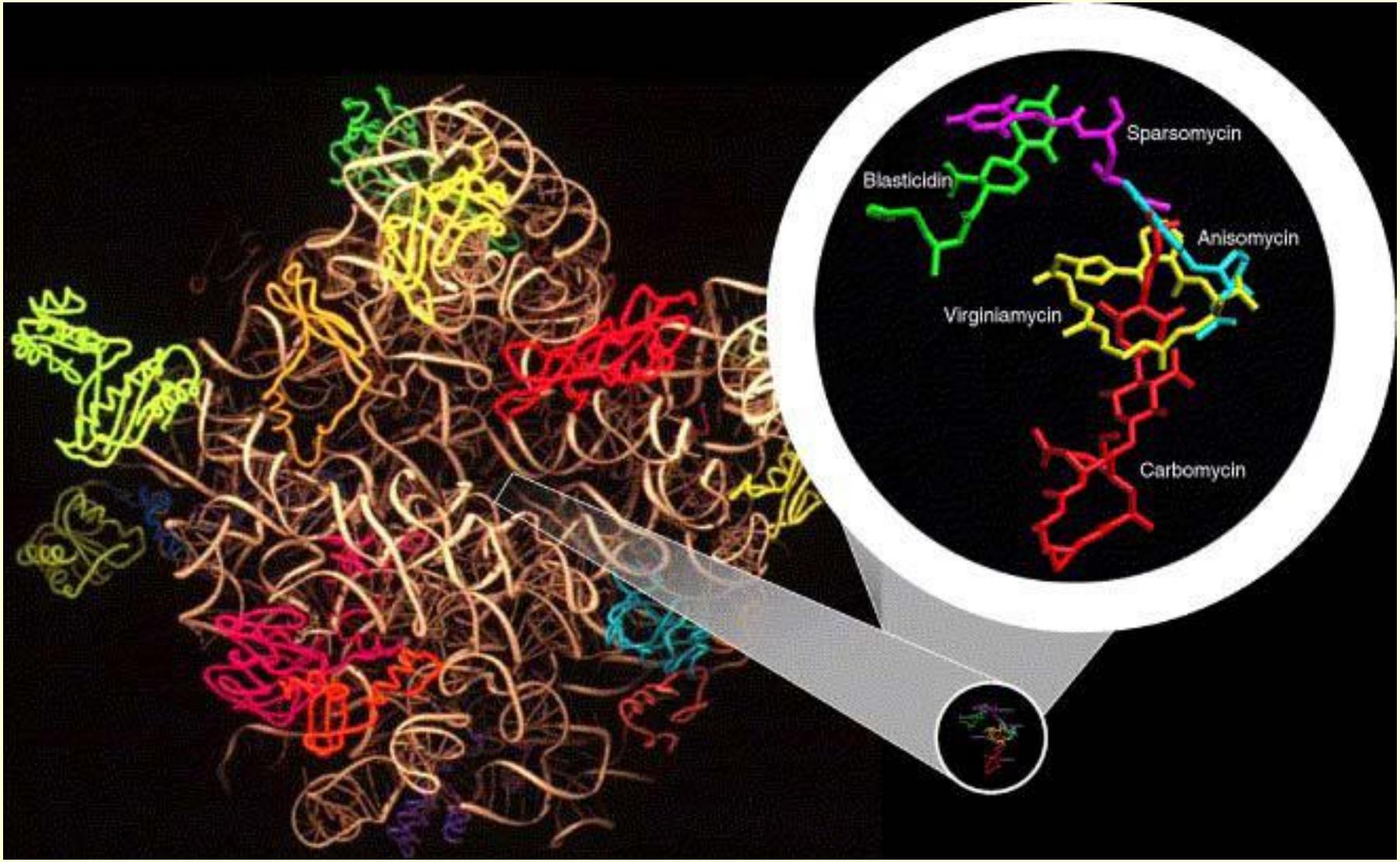

The peptidyl-transferase center in the 50S ribosomal subunit is attacked by a large number of existing antibiotics, now revealed at high resolution in 50S subunit crystal structures (Figure 8) (Franceschi and Duffy, 2006).